AN ABSTRACT OF THE THESIS OF

Grant Masaru Yoshihara for the degree of Master of Science
(Name)

in Nuclear Engineering presented on June 19, 1979
(Major) (Date)

Title: CALCULATION OF CONSISTENT STEADY-STATE CONDITIONS FOR BOILING WATER REACTORS BASED ON RETRAN MODELS

Redacted for Privacy

Abstract approved: K. Hornyik

A study regarding steady-state conditions in boiling water reactors was conducted in order to provide consistent initial conditions for transient analysis using the computer simulation code, RETRAN. Consistent steady states were generated with the RETRAN model of the system by first establishing a reference state, and then obtaining other steady states as asymptotic equilibria which the system approaches some time after introducing certain perturbations. A simplified version of the RETRAN model was then used as the basis for the development of an approximate explicit solution, based on steady-state mass and momentum conservation, to predict the asymptotic flow rates in the reactor vessel as a function of the recirculation pump speed. The results from these calculations were compared to the equilibrium conditions determined by the RETRAN calculations, sources of error were examined, and conclusions were drawn.

The analysis demonstrated that the method used to predict the flows and pump speed at various steady-state conditions provides good agreement with the RETRAN results. An error analysis indicated that errors due to the approximations generally increased as the strength of the perturbation increased (i.e., increased deviation from the reference state). However, the magnitude of the errors is such that, within limitations, the simple model provides good approximations of the flows and pump speed which are consistent with the RETRAN model.

The advantage of the explicit solution obtained by the simplified model lies in the fact that it permits direct and easy determination of steady-state system flow rates when pump speed and reactor power are given. When these flow rates are used as input to RETRAN, they will result in the determination of junction form loss coefficients for closed flow loops which will closely match those of the reference state, hence the condition for consistency is satisfied.

Calculation of Consistent Steady-State Conditions for Boiling Water Reactors Based on RETRAN Models

by

Grant Masaru Yoshihara

A THESIS

submitted to

Oregon State University

in partial fulfillment of

the requirements for the

degree of

Master of Science

Commencement June 1980

APPROVED:

Redacted for Privacy

Associate Professor of Nuclear Engineering

Redacted for Privacy

Head of Nuclear Engineering Department

Redacted for Privacy

Dean of Graduate School

Date thesis is presented June 19, 1979

Typed by Cheryl E. Curb for Grant Masaru Yoshihara

ACKNOWLEDGEMENTS

I wish to express my sincere thanks to my friend and advisor, Dr. Karl Hornyik, for his advice, knowledge, and guidance. I would also like to thank the Electric Power Research Institute, along with Dr. Bal Raj Segal, and Dr. Joseph A. Naser, for supporting my graduate studies. Finally, I would like to recognize Dr. Bernard I. Spinrad, my undergraduate advisor, who helped me make many decisions about my education.

I dedicate this thesis to my parents, who have supported me in all my educational endeavors.

TABLE OF CONTENTS

LIST OF ILLUSTRATIONS

LIST OF TABLES

CALCULATION OF CONSISTENT STEADY-STATE CONDITIONS FOR BOILING WATER REACTORS BASED ON RETRAN MODELS

I. INTRODUCTION AND OBJECTIVES

Transient analysis is an important aspect in evaluating the performance of nuclear steam supply systems. By examining the plant response to system perturbations, the ability of the plant to remain within the bounds of safe operation can be ascertained. Currently transient analysis is performed with elaborate computer simulation codes, partially supported by experimental evidence obtained from small scale test loops and operating plants.

Computer simulation codes are based on analytic models which are formulations of relevant physical laws and engineering principles, and require as input the physical characteristics of the system as well as initial and boundary conditions. Nuclear, mechanical, and thermodynamic material properties, and mechanical systems performance data also are often part of the input. The initial values of the system variables need to be chosen in a manner consistent with the analytical model so that they constitute the initial equilibrium level. Such an equilibrium is commonly postulated to exist prior to the initiation of a transient.

The initial values for system variables are found by solving the steady-state formulations of the equations which describe the system. This includes determination of the fluid conditions throughout the nuclear steam supply system based on conservation of mass,

energy, and momentum, component temperatures based on heat transfer laws, and other variables which play a role in the steam production process, such as reactor power, pump parameters, and control system signals. For instance, as part of the initial steady-state analysis, the system pressure drops can be determined as a function of the fluid flow rates, which are assumed to be known. Due to the non-linear nature of the equations, this will generally require an iterative process. Thus, given a set of input data necessary and sufficient to define a unique state of the system, the variables characterizing this state can be determined. On the other hand, there is no unique choice with regard to the input set, and it is often a matter of calculational convenience that decides which quantities are considered as input and which are to be determined by the steady-state balance.

Actual control of the plant operating state is carried out through certain means which change the level of heat production in the reactor core. The two methods used in controlling the power level of boiling water reactors are adjusting control rod positions, and changing the amount of flow through the recirculation system. The latter method works through the relationship between recirculation flow and steam void fraction in the core zone. This, in turn, has a strong effect on reactivity and thus, on the power level.

The settings of these means of control (rod positions, recirc. pump speed) along with certain other conditions (e.g., feedwater enthalpy, pressure controller and level controller set points) constitute the set of input parameters which uniquely determine the

steady-state from the operator's point of view. As is the case in this study, this set is different from the set required by the computer code used for simulation of the plant. This means that a trial and error procedure may have to be used to determine the input, as required by the code, which achieves the desired steady-state determined at the operating plant. This process can be tedious and time consuming when attempting to develop several different sets of input at various plant operating levels, as is usually needed when studying a wide range of conditions.

A related problem is that of assuring agreement between calculated and measured steady-states over all possible plant conditions of interest. Often one can achieve agreement at a reference condition (e.g., nominal full power) by adjusting certain model parameters, in particular those which are associated with a high degree of uncertainty. However, agreement at this reference condition does not guarantee that other states which are reached from it by introducing operational system changes also will be in agreement with measured counter parts. Deviations may be due to improper values of relevant system parameters, overly simplistic models, truncation, and other approximations in the numerical methods used to solve the model equations. Last but not least, errors may exist in the measurement and/or interpretation of plant parameters.

The objective of this thesis is to resolve the problem of determination of consistent steady-state conditions as outlined above. The computer simulation model underlying this study is the RETRAN code package as applied to the modeling of a boiling water reactor

(BWR). Specifically, an explicit functional relationship is derived from RETRAN fluid flow equations between the recirculation pump speed and the steady-state flow rates in the pressure vessel and recirculation loops of a BWR. This relationship can be used to directly determine consistent steady-state flow rates as required by RETRAN when the recirculation pump speed is given. Although the same goal can be reached by trial and error, use of the method presented here will be significantly more convenient and less costly. In addition, the results of this work can be used to compare computed and measured steady-state conditions over a wide range. Due to the explicit and relatively simple nature of the relations which are developed, it then appears easy to eliminate eventual discrepancies by suitable adjustment of certain model parameters.

The remainder of this thesis is organized as follows: First, brief descriptions are given of a typical BWR and of the RETRAN code. Then the details of the derivation of the explicit steady-state relation between flow rates and recirculation pump speeds are presented. These derivations start from the steady-state momentum equations as used in RETRAN which relate flow rates and pressure drops for all relevant flow paths throughout the model. They also involve the pressure increase developed by the recirculation pumps. This pressure increase in turn is related to other pump characteristics such as flow rate and speed by way of empirically determined relations (homologous pump curves). Approximations are then introduced as needed in order to obtain a workable set of equations, and the final relationships are developed relating the pump speed

directly to major flow variables. The results of this simplified model, along with those corresponding calculations performed with the RETRAN code, are presented in Chapter IV. Conclusions are drawn and limitations of this approach to predicting the steady-state flows are presented in Chapter V. A complete listing of the nomenclature used throughout this thesis, details of the approximations for the pump curves as well as other details of derivations, and an input listing of a sample calculation are relegated to the Appendices.

II. BACKGROUND INFORMATION

A. Boiling Water Reactor Description

A description of the important features of the BWR nuclear steam supply system (NSSS) pertinent to the following analysis is presented here. A general description of the BWR can be found in a number of literature (e.g., Reference 1). It is important to note that the following design description applies to the BWR/4 plant design, as subsequent newer BWR designs have several different features.

The basic BWR flow model is shown in Figure 1. Water, which serves both as a neutron moderator and coolant, flows through the nuclear core where some of it is converted to steam. This steam is separated from saturated water and is dried in the upper internals of the pressure vessel. It leaves the vessel to drive the turbine generators, is condensed, demineralized, and returns to the vessel through feedwater pumps and heaters. The saturated water emerging from the steam separators and driers is returned to the core by way of the downcomer and the recirculation system as described in the next paragraph.

The BWR features high performance jet pumps located within the reactor vessel, as shown in Figure 2. The driving flow for the jet pumps is provided by a two-loop recirculation system with two recirculation pumps taking suction from the lower downcomer. The flow emerging from the recirculation pumps under increased pressure is redistributed to a manifold outside the pressure vessel and

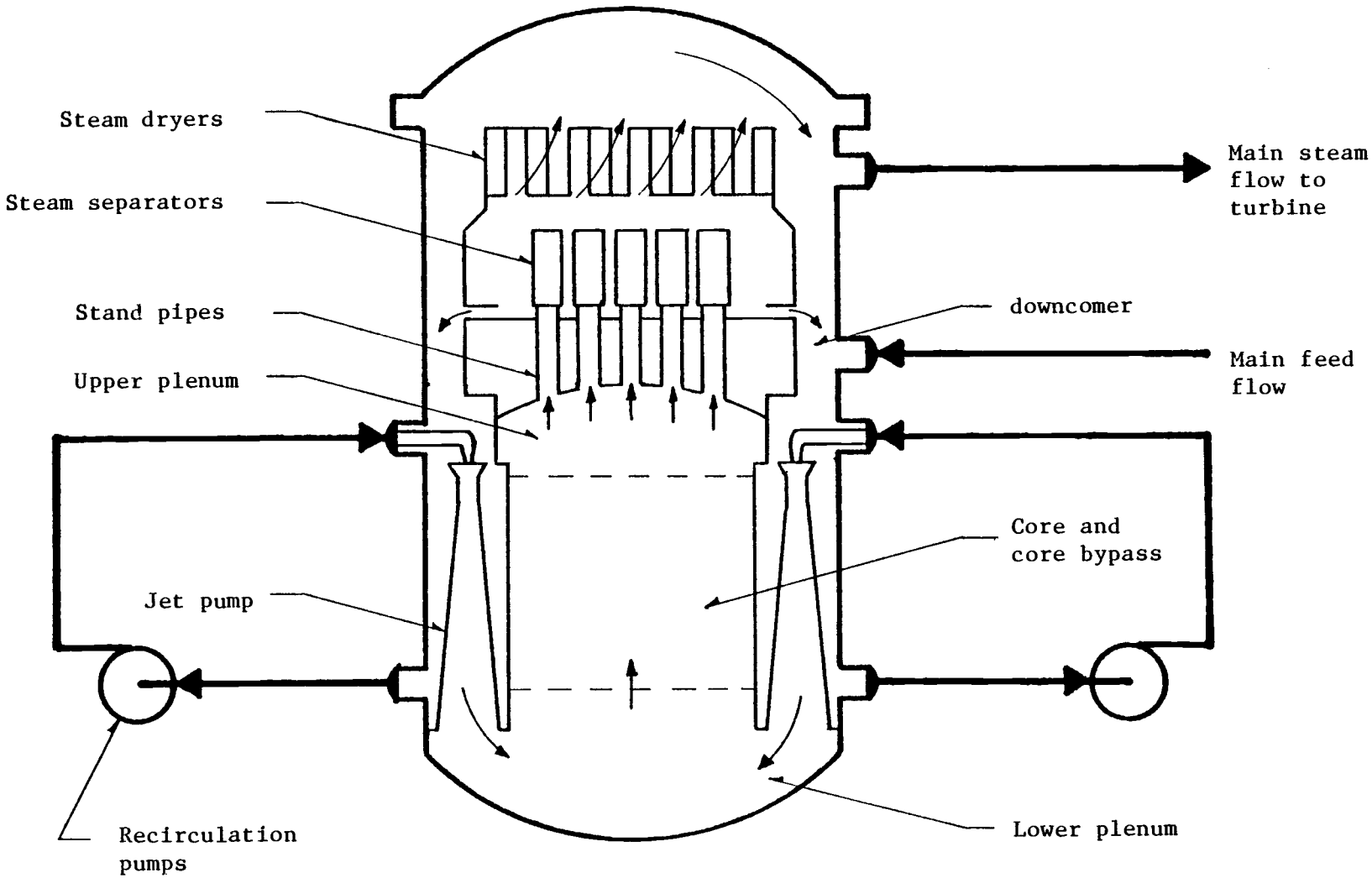

Figure 1. Steam and Recirculation Water Flow in a boiling water reactor.

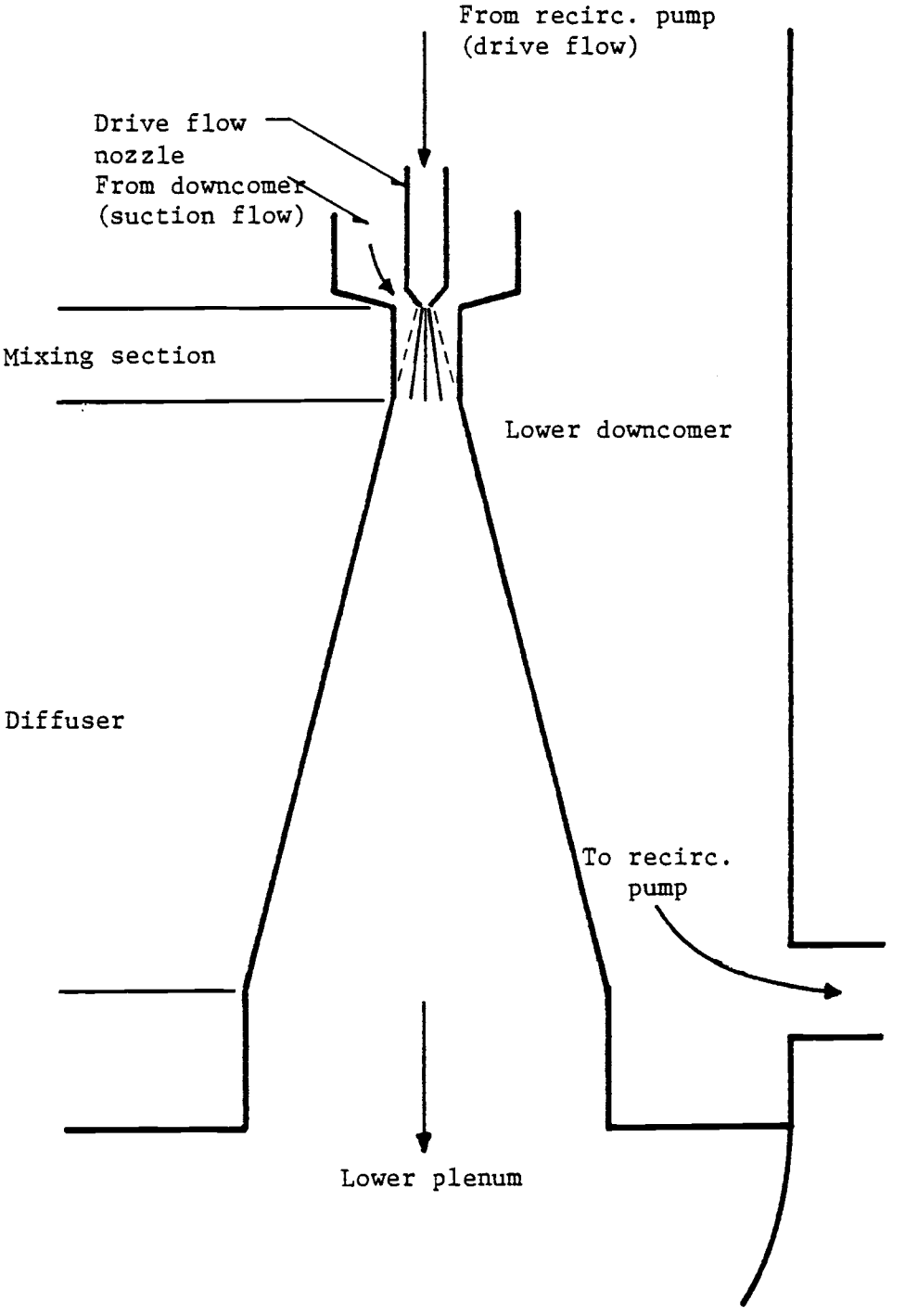

Figure 2. BWR Jet Pumps

discharged through jet pump nozzles into 16 to 24 jet pumps, depending on the size of the plant. The drive flow induces water in the downcomer to be drawn into the jet pump throat by momentum transfer and the two flows mix, then diffuse in the diffuser section, discharging into the lower plenum. This jet pump drive system uses high pressure flow accelerated to high speed mixing with a low pressure flow to create a dynamic head which is converted to a static head in the diffuser to provide forced circulation through the reactor core.

Reactor control is enhanced by the use of the jet pump recirculation system. Variable speed recirculation pumps are used to change the recirculation flow. A decrease in the drive flow to the jet pumps is accompanied by a reduction in the total flow through the core. This causes a decrease in the cooling water density in the core, since a lower mass flow rate removing the same amount of heat will cause an increase in the void content. At the same time, fewer water molecules are available for the slowing down of fast neutrons to thermal energies, a basic requirement for thermal fission. Hence, the thermal neutron flux decreases, resulting in a decrease in the heat generated by the nuclear core, and an overall reduction in power level.

The jet pump recirculation system provides the BWR with good load-following capability. Coupled with the use of conventional control rod positioning characteristic to all nuclear generating systems, the BWR has the ability to easily change the level of steam production to meet required generation demands, as shown in Figure 3. This power-flow map charts the core thermal power versus

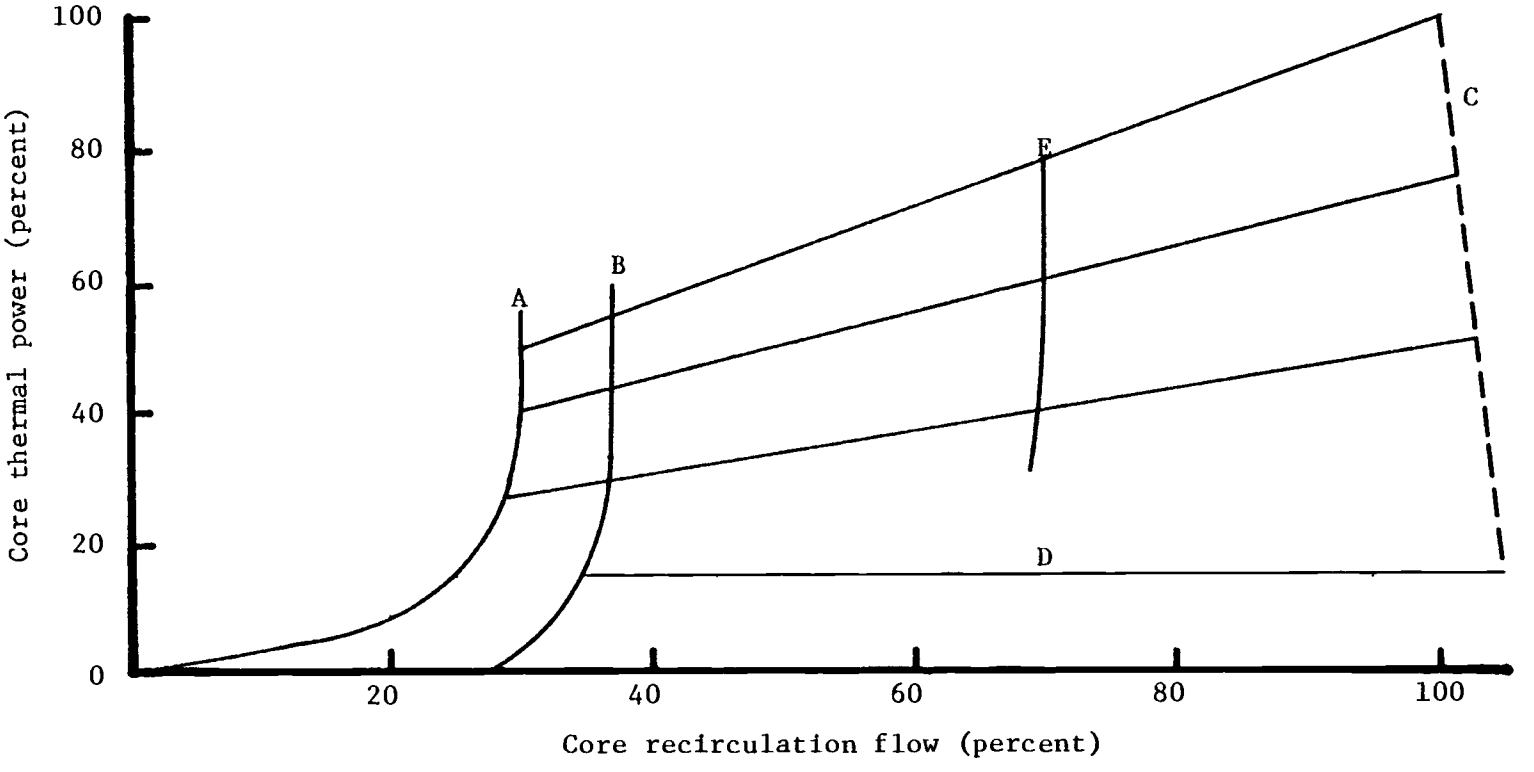

(a) natural circulation
(b) 20% pump speed
(c) pump speed for full flow @ full power
(d) low feedwater recirculation runback limit
(e) rated flow control line

Figure 3. Sample BWR Power-Flow Map

the total or core recirculation flow. As shown, the reduction of the recirculation pump speed with fixed control rod positions brings the thermal power and core recirculation flow down along flow control lines. Control rod movement changes the core thermal power while effecting only minor changes in the total core recirculation flow under constant recirculation pump speed.

The power-flow map also demonstrates another characteristic of BWR's. The generation of steam within the reactor vessel results in a very strong buoyancy force which basically enables the BWR to operate on natural circulation up to 50% power.

The BWR/4 plant characteristics used for the reactor model are taken from the Peach Bottom Atomic Generating Station Unit 2. The plant is rated at 3293 MW thermal output, 102.5 x 10^6 lb/hr core flow, and 13.37 x 10^6 lb/hr steam flow at 965 psia turbine inlet pressure. Further information on the Peach Bottom Unit 2 plant including basic design information and operating history is available in References 1 and 2.

Additional design and performance data was recorded during a series of transient and stability tests which were conducted at the Peach Bottom Plant in April, 1977. This information is found in Reference 3. Specific plant characteristics for the computer model input used for the simulation of the aforementioned tests are found in Reference 4.

B. RETRAN Description

The RETRAN (RElap4 TRANsient) system analysis code was developed to simulate the thermal-hydraulic behavior of light-water reactors during operational transients and normal startup and shutdown operations. It contains essentially the same thermal-hydraulic differential and state equations as employed in the RELAP4 simulation code. Whereas a full description of the RETRAN code package is found in Reference 5, this presentation is concerned only with those portions of the code which are pertinent to this thesis.

To describe the behavior of the fluid in the relevant flow systems of a plant, these flow systems are broken down into a linear network of volumes suitably connected by junctions. The conservation principles of mass, energy, and momentum, and the fluid state equations are applied to each volume or junction in terms of volume averaged state variables and flow characteristics. Empirical correlations are required for describing specific phenomena such as single and two-phase friction, boiling heat transfer, critical flow calculations, and others.

Code submodules for the simulation of pumping systems, heat exchangers, and other mechanical equipment are necessary for modeling of special components commonly found in light water reactors. Of prime importance to this particular study are the centrifugal pump model, jet pump momentum transfer formulation, and the steady-state self initialization option.

The pump model, which describes the pump performance in fluid systems, uses pump characteristic curves derived from empirical data

generally supplied by the pump manufacturer. The curves represent functional relations between pump head, flow, speed, and torque data in tabular form. Linear interpolation is used between data points to approximate continuous functional relationships (see Appendix B).

Special formulations of the momentum equations are used for modeling of two-stream fluid mixing as is essential in jet pump action. These formulations are presented in Chapter III. The suction and drive flow paths are modeled as separate junctions, with momentum exchange in the throat of the jet pump represented in the momentum equation for both junctions.

The steady-state self initialization option allows the user to provide a minimum of input data which is sufficient to define the state of the system. The code then employs an iterative process to calculate a complete steady-state set of initial values for the remaining system variables. Specific requirements of this option are the specification of all junction flow rates satisfying conservation of mass requirements, one enthalpy and one pressure per flow system, and all junction form loss coefficients with the exception of one loss coefficient for each closed loop flow path, along with all of the geometric system parameters. The code will then calculate values for the unspecified loss coefficient(s) which satisfy closed loop pressure conditions in steady-state. Alternatively, the user may specify all volume pressures and junction flow rates, and one enthalpy per flow system, and have the code generate all the loss coefficients, or any combination of volume pressures and junction loss coefficients. Regardless of any of the aforementioned

options, the junction flow rates and geometric system parameters, with the exception of the loss coefficients, must be specified.

When applying the RETRAN code to model a given system, one faces the problem of having to specify quantities which are actually process variables. On the other hand, the code, in order to achieve equilibrium conditions, will calculate quantities which actually are system characteristics. This can lead to a number of difficulties, such as obtaining unrealistic or inconsistent values for these parameters when applying the code to several different equilibrium states of the same system. A more proper approach would be to balance the system by solving for the junction flow rates, since empirical data are available for specifying the loss coefficients. However, this results in a substantial increase in the numerical complexity due to the second-order flow terms.

Whereas steady-state self initialization is recognized as an important feature of RETRAN, it appears that the current version does not permit specification of those parameters which are used in an operational sense to define a steady state. The analysis outlined in the subsequent chapters presents a solution to this problem. For the case of BWR's, the solution is obtained in the form of explicit relations for the determination of flow rates from (known) system parameters, in particular, pump speed and geometric parameters. Since these equations are derived from the RETRAN flow equations applied to a typical BWR, the solution is fully consistent with RETRAN except for minor deviations introduced by making a number of simplifying assumptions.

C. RETRAN Boiling Water Reactor Model

The RETRAN model used as the basis for the steady-state analysis presented in this thesis is shown in Figure 4. This model was devised for simulation of the Peach Bottom Unit #2 turbine trip tests (Reference 4). Thirty-five (35) volumes represent the vessel internals, recirculation loops, and steam lines. Single flow paths are used whenever two or more parallel flow paths have identical characteristics. A full description is found in the aforementioned reference. The model was used to determine a set of consistent steady states, by first establishing a reference 100% power, 100% core reculation flow (refer to Figure 3), then introducing changes in pump speed and/or control rod position. In each case, the new steady-state condition was obtained as the asymptotic equilibrium which is approached some time after introducing the perturbation.

A simplified model is shown in Figure 5. This was done to reduce the mathematical complexity of the steady-state relationships, and to eliminate portions of the full model that are not essential to this analysis. The major simplification pertains to the reactor core region, where a single, lumped volume replaces the 12 volume core model previously used. The steam line is eliminated as the steam flow can be determined by the flows within the pressure vessel. Also, flow from the exterior portion of the steam separator (Figure 4, Volume 34) to the steam dome dryer (Figure 4, Volume 35) is neglected due to its small magnitude (approximately 2 lbm/sec) and the steam dome dryer and steam dome volumes are consolidated into one volume. This simplified model is used as the basis for defining

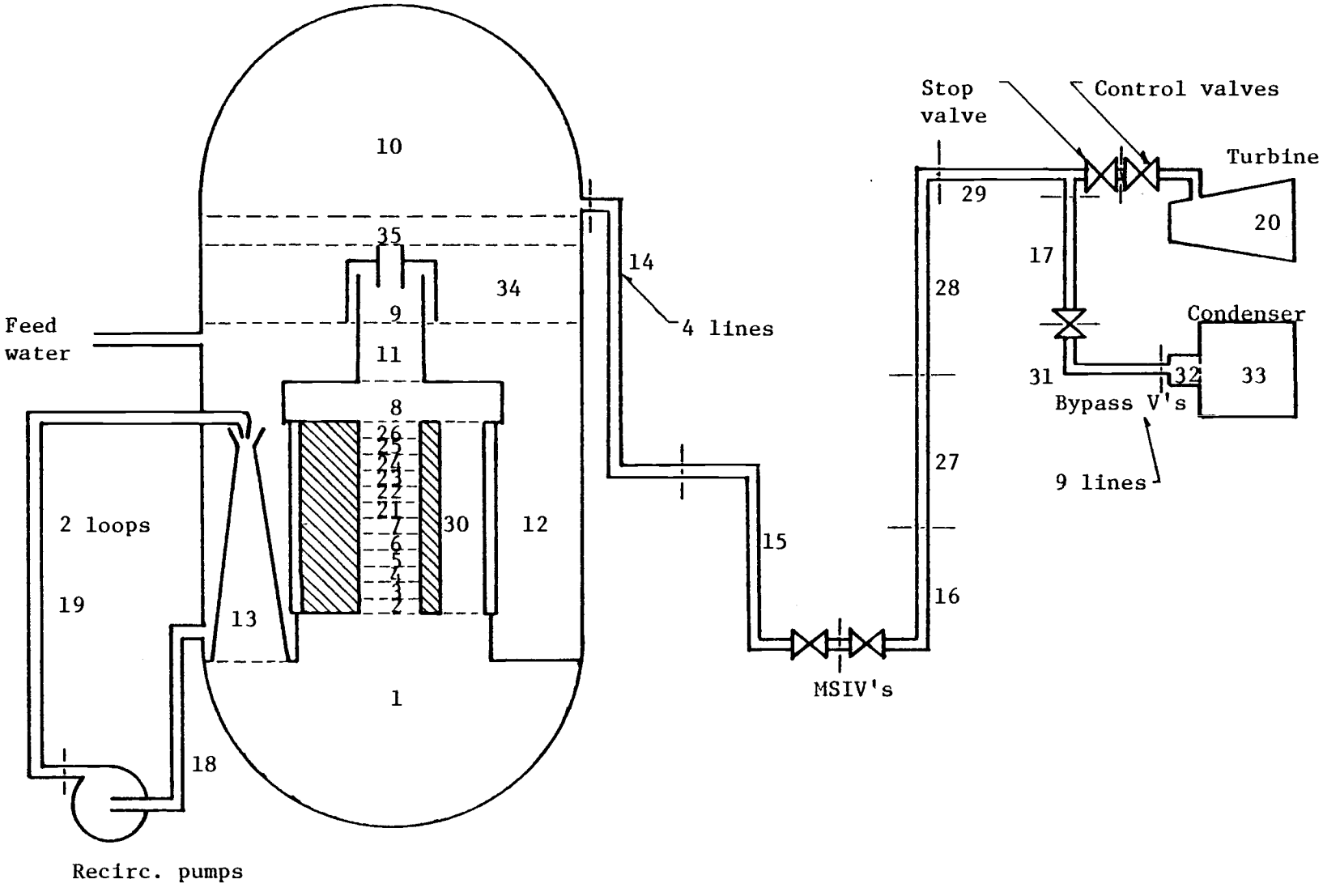

Figure 4. RETRAN Model of a boiling water reactor.

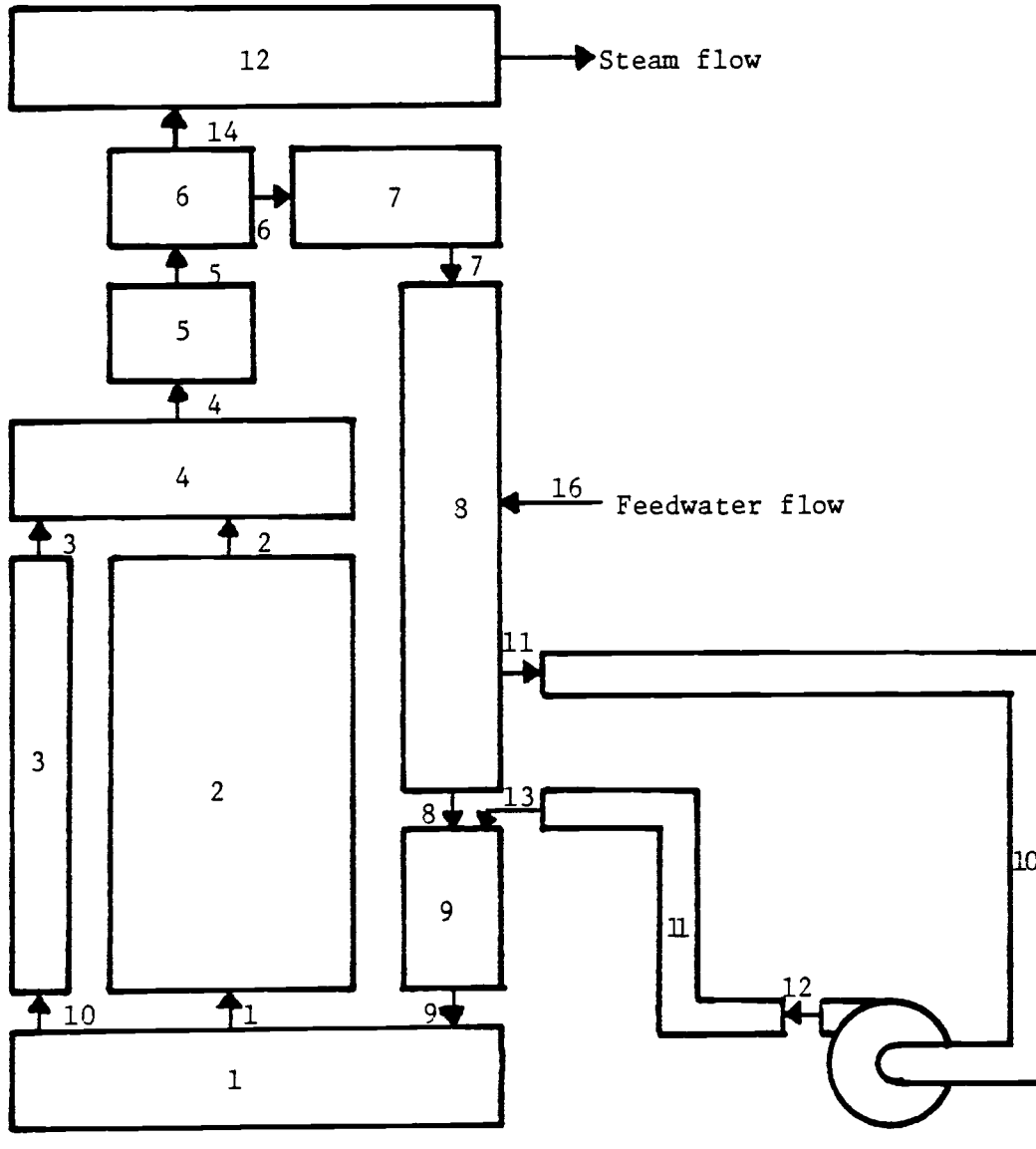

(1) lower plenum
(2) core
(3) core bypass
(4) upper plenum
(5) stand pipes
(6) steam separator
(7) steam separator exterior
(8) downcomer
(9) jet pumps
(10) recirc. suction line and pump
(11) recirc. discharge line
(12) steam dome and steam dome drier

Figure 5. Schematic of the Simplified RETRAN-BWR Model.

the steady-state relationships required to formulate the flow versus pump speed approximation. The model contains three closed loops; (1) the reactor core and core bypass, (2) the reactor vessel through the core, upper internals, downcomer, jet pumps, and lower plenum, and (3) the recirculation loop through the recirculation pumps and jet pumps. These are referred to as the core, vessel, and recirculation loops, respectively, for the remainder of the text.

III. STEADY-STATE ANALYSIS

A. Steady-State Momentum Equations

At steady-state equilibrium, the pressure drop between two adjacent connected volumes (see Figure 6) is obtained by RETRAN on a volume average basis from applying the conservation of momentum law:

$$P_l - P_k = \frac{1}{144 g_c}\left[\frac{\bar{W}_k^2}{\bar{\rho}_k \bar{A}_k^2} - \frac{\bar{W}_l^2}{\bar{\rho}_l \bar{A}_l^2} - \frac{W_j^2}{2\bar{\rho}_j}\left(\frac{1}{\bar{A}_k^2} - \frac{1}{\bar{A}_l^2}\right)\right.$$

$$-\left(\frac{f_k l_k \phi_k \bar{W}_k^2}{D_{hk} \bar{\rho}_k \bar{A}_k^2} + \frac{f_l l_l \phi_l \bar{W}_l^2}{D_{hl} \bar{\rho}_l \bar{A}_l^2}\right) - \frac{K_j W_j^2}{2 \rho_j A_j^2}$$

$$\left. + g_o\left(\bar{\rho}_k(\bar{z}_k - z_j) + \bar{\rho}_l(z_j - \bar{z}_l)\right)\right] \qquad \text{(III-1)}$$

where the subscripts k, l and j refer to conditions at the upstream volume, downstream volume, and connecting junction, respectively. The bar superscript refers to volume average conditions. The notation used here is that of Reference 5, and is explained in Appendix A. Equation (III-1) is applied to all junctions of the model with the exception of four junctions; the junctions on either side of the recirculation pump volume, where one-half of the pump differential pressure is added to each junction, and the jet pump junctions.

The jet pump suction and drive flow junctions require a special formulation of the momentum equation for modeling two-stream fluid mixing (refer to Reference 6). Figure 7 shows the schematic pertinent to the jet pumps. The mixing section is not represented

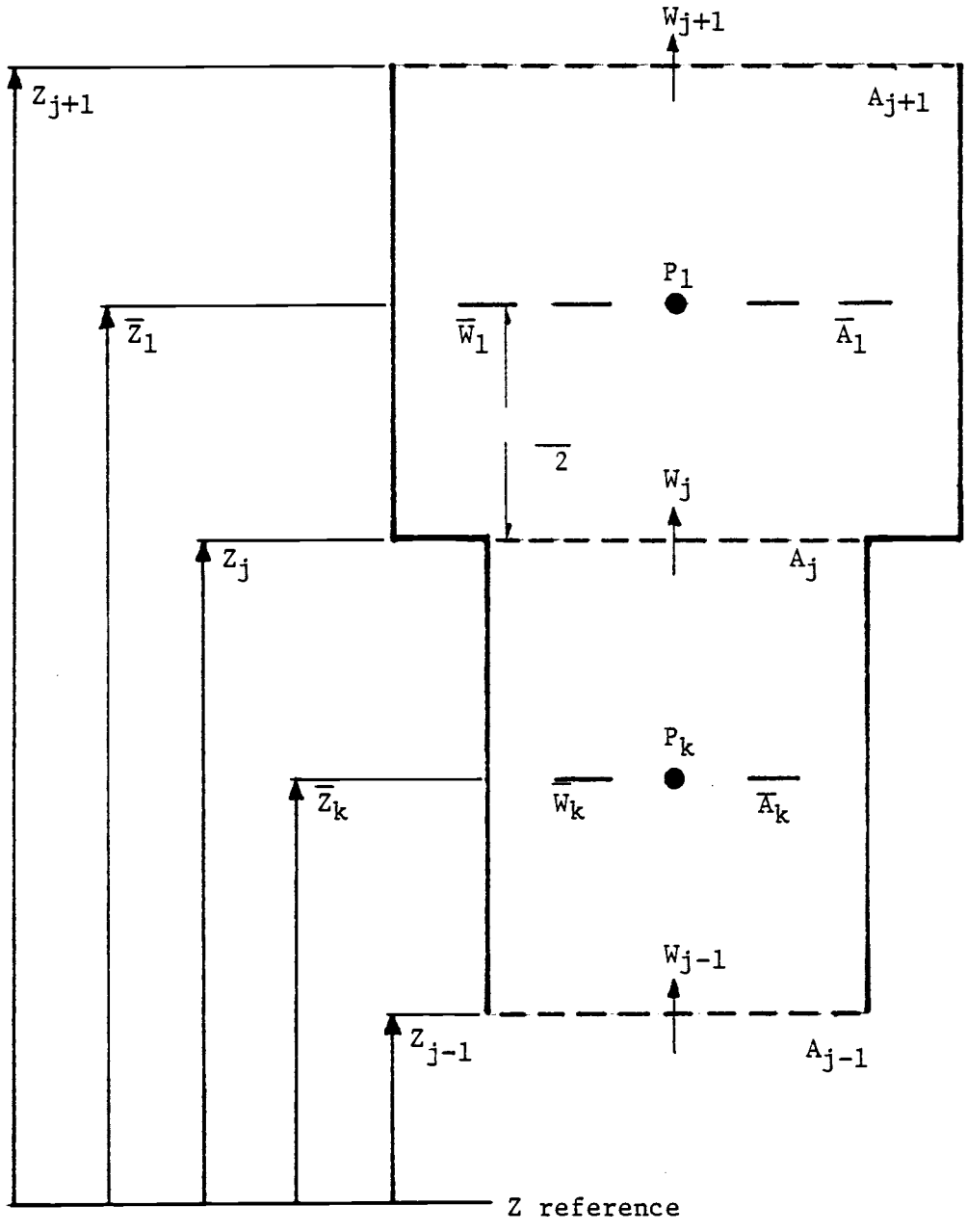

Figure 6. Schematic of a RETRAN Junction Connecting Two Volumes.

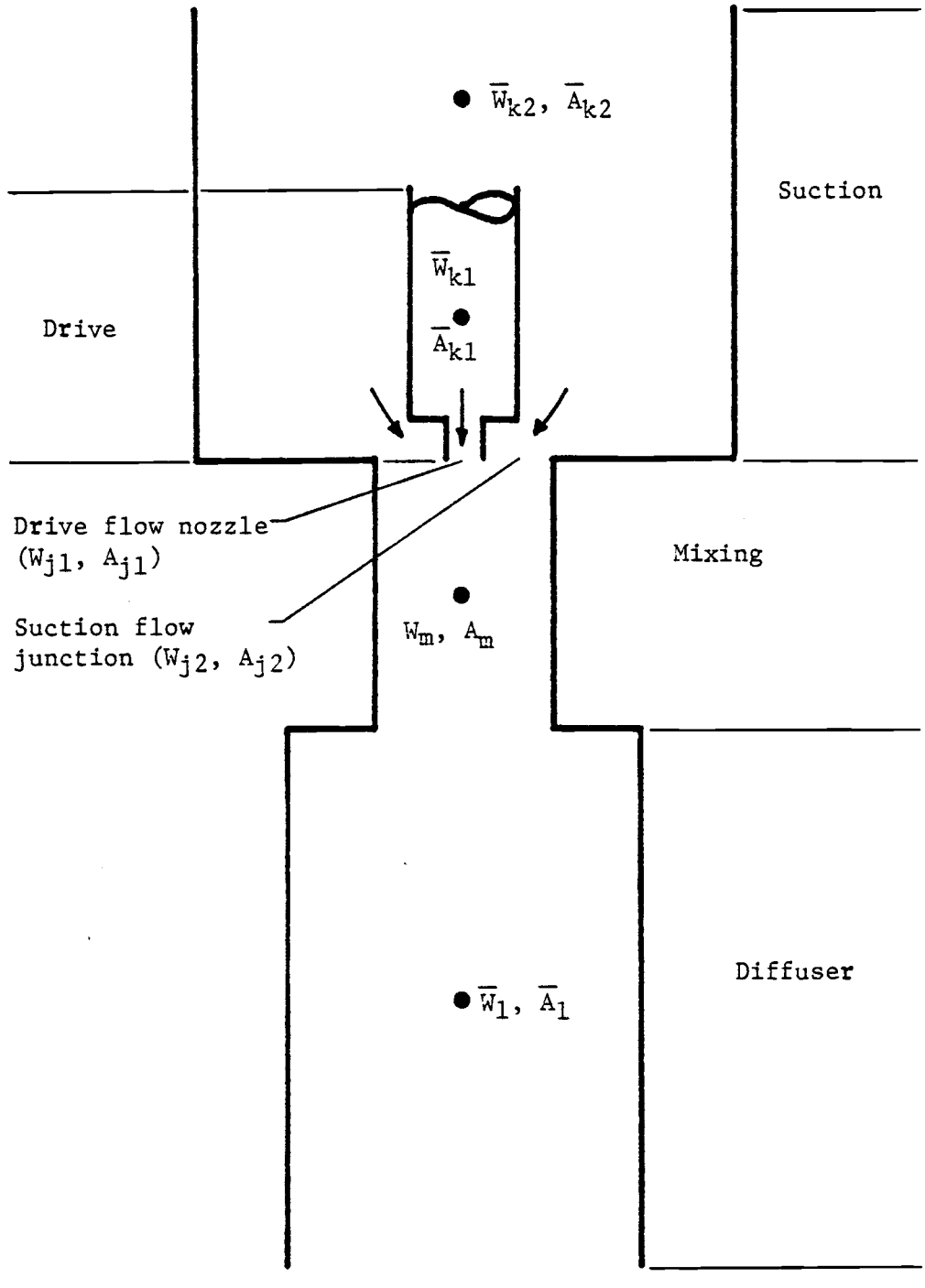

Figure 7. Schematic of the RETRAN Jet Pump Model.

as a separate RETRAN volume, but rather is incorporated directly into the junction equation as given below.

Under steady-state equilibrium conditions, the momentum equation for the drive flow junction is

$$P_l - P_{k1} = \frac{1}{144\,g_c}\left[\frac{W_{j1}^2}{2\rho_{j1}}\left(\frac{1}{\bar{A}_{k1}^2} - \frac{1}{A_{j1}^2}\right) + \frac{W_m^2}{2\rho_m}\left(\frac{1}{A_m^2} - \frac{1}{\bar{A}_l^2}\right)\right.$$

$$+ \frac{W_{j1}V_{j1} + W_{j2}V_{j2} - W_mV_m}{A_m} - \left(\frac{f_{k1}l_{k1}\phi_{k1}\bar{W}_{k1}^2}{D_{hk1}\bar{\rho}_{k1}\bar{A}_{k1}^2} + \frac{f_l l_l \phi_l \bar{W}_l^2}{D_{hl}\bar{\rho}_l \bar{A}_l^2}\right)$$

$$\left. - \frac{K_{j1}W_{j1}^2}{2\rho_{j1}A_{j1}^2} + g_o\left(\bar{\rho}_{k1}(\bar{z}_{k1} - z_{j1}) + \bar{\rho}_l(z_{j1} - \bar{z}_l)\right)\right]$$

where the subscripts j1 and j2 refer to the drive and suction flow junctions, respectively, and subscripts 1 and k1 refer to the volumes connected by the drive flow junction. For the suction flow junction,

$$P_l - P_{k2} = \frac{1}{144\,g_c}\left[\frac{\bar{W}_{k2}^2}{\bar{\rho}_{k2}\bar{A}_{k2}^2} - \frac{W_{j2}^2}{\bar{\rho}_{j2}\bar{A}_{j2}^2} + \frac{W_{j2}^2}{2\rho_{j2}}\left(\frac{1}{A_{j2}^2} - \frac{1}{\bar{A}_{k2}^2}\right)\right.$$

$$+ \frac{W_m^2}{2\rho_m}\left(\frac{1}{A_m^2} - \frac{1}{\bar{A}_l^2}\right) + \frac{W_{j1}V_{j1} + W_{j2}V_{j2} - W_mV_m}{A_m}$$

$$- \left(\frac{f_{k2}l_{k2}\phi_{k2}\bar{W}_{k2}^2}{D_{hk2}\bar{\rho}_{k2}\bar{A}_{k2}^2} + \frac{f_l l_l \phi_l \bar{W}_l^2}{D_{hl}\bar{\rho}_l\bar{A}_l^2}\right) - \frac{K_{j2}W_{j2}^2}{2\rho_{j2}A_{j2}^2}$$

$$\left. + g_o\left(\bar{\rho}_{k2}(\bar{z}_{k2} - z_{j2}) + \bar{\rho}_l(z_{j2} - \bar{z}_l)\right)\right]$$

where the j1 and j2 subscripts are retained and the 1 and k2 subscripts now refer to the volumes connected by the suction flow junction. Subscript m refers to the mixing section of the jet pump, and is defined to be the sum total of the drive and suction flow junction conditions for the junction areas and flows, and the density averaged over the two streams.

Referring to Figure 5, the simplified volume model, the following mass flow rate relationships must be satisfied as based on steady-state mass balances for the three closed loops in the system (see Appendix A for definitions):

$$W_t = W_d + W_s \qquad \text{(III-4)}$$

$$W_t = W_c + W_b \qquad \text{(III-5)}$$

$$W_t = W_r + W_p \qquad \text{(III-6)}$$

The steam flow leaves the steam separator and passes through the steam dome, leaving the vessel through junction 15 in Figure 5. The recirculation flow (in Equation III-6) is that portion of the total flow which is separated from the steam and recycled back through the downcomer. The total flow and the core recirculation flow are one and the same, and further reference to this quantity will be designated W_t, the total flow.

B. Flow Loop Equations

The momentum relationships can be written for all junctions of the three loops of the flow model. The boundary conditions which apply to this system require that the pressure drops summed over each of the three closed loops must be equal to zero.

For the core flow loop, this condition can be written as

$$W_b^2\left[\frac{1}{2\rho_{10}}\left(\frac{1}{\bar{A}_1^2}-\frac{1}{\bar{A}_3^2}\right)+\frac{1}{2\rho_3}\left(\frac{1}{\bar{A}_3^2}-\frac{1}{\bar{A}_4^2}\right)+\frac{2f_3\ell_3\phi_3}{D_{h_3}\bar{\rho}_3\bar{A}_3^2}+\frac{K_{10}}{2\rho_{10}A_{10}^2}+\frac{K_3}{2\rho_3A_3^2}\right]$$

$$-W_c^2\left[\frac{1}{2\rho_1}\left(\frac{1}{\bar{A}_1^2}-\frac{1}{\bar{A}_2^2}\right)+\frac{1}{2\rho_2}\left(\frac{1}{\bar{A}_2^2}-\frac{1}{\bar{A}_4^2}\right)+\frac{2f_2\ell_2\phi_2}{D_{h_2}\bar{\rho}_2\bar{A}_2^2}+\frac{K_1}{2\rho_1A_1^2}+\frac{K_2}{2\rho_2A_2^2}\right]$$

$$+g_0\left[\bar{\rho}_2(Z_1-Z_2)-\bar{\rho}_3(Z_{10}-Z_3)\right]=0$$

where terms for the flow rates W_b and W_c have been separated from the gravitational terms.

Examining the vessel loop in a similar manner and using Equation (III-2) for the suction flow junction results in a relationship including the total flow (W_t), core flow (W_c), suction flow (W_s), drive flow (W_d), and recirculation flow (W_r):

$$W_t^2\left[\frac{1}{2\rho_m}\left(\frac{1}{A_m^2}-\frac{1}{\bar{A}_9^2}\right)-\frac{1}{2\rho_4}\left(\frac{1}{\bar{A}_4^2}-\frac{1}{\bar{A}_5^2}\right)-\frac{1}{2\rho_5}\left(\frac{1}{\bar{A}_5^2}-\frac{1}{\bar{A}_6^2}\right)-\frac{1}{2\rho_9}\left(\frac{1}{\bar{A}_9^2}-\frac{1}{\bar{A}_1^2}\right)\right.$$

$$+\frac{1}{\rho_9\bar{A}_9^2}-\frac{1}{\rho_m A_m^2}-\frac{2f_1 l_1\phi_1}{D_{h_1}\bar{\rho}_1\bar{A}_1^2}-\frac{2f_4 l_4\phi_4}{D_{h_4}\bar{\rho}_4\bar{A}_4^2}-\frac{2f_5 l_5\phi_5}{D_{h_5}\bar{\rho}_5\bar{A}_5^2}-\frac{2f_6 l_6\phi_6}{D_{h_6}\bar{\rho}_6\bar{A}_6^2}$$

$$\left.-\frac{2f_8 l_8\phi_8}{D_{h_8}\bar{\rho}_8\bar{A}_8^2}-\frac{2f_9 l_9\phi_9}{D_{h_9}\bar{\rho}_9\bar{A}_9^2}-\frac{K_4}{2\rho_4 A_4}-\frac{K_5}{2\rho_5 A_5^2}-\frac{K_9}{2\rho_9 A_9^2}\right]$$

$$-W_c^2\left[\frac{1}{2\rho_1}\left(\frac{1}{\bar{A}_1^2}-\frac{1}{\bar{A}_2^2}\right)+\frac{1}{2\rho_2}\left(\frac{1}{\bar{A}_2^2}-\frac{1}{\bar{A}_4^2}\right)+\frac{2f_2 l_2\phi_2}{D_{h_2}\bar{\rho}_2\bar{A}_2^2}+\frac{K_1}{2\rho_1 A_1^2}+\frac{K_2}{2\rho_2 A_2^2}\right]$$

$$-W_r^2\left[\frac{1}{2\rho_6}\left(\frac{1}{\bar{A}_6^2}-\frac{1}{\bar{A}_7^2}\right)+\frac{1}{2\rho_7}\left(\frac{1}{\bar{A}_7^2}-\frac{1}{\bar{A}_8^2}\right)+\frac{2f_7 l_7\phi_7}{D_{h_7}\bar{\rho}_7\bar{A}_7^2}+\frac{K_6}{2\rho_6 A_6^2}+\frac{K_7}{2\rho_7 A_7^2}\right]$$

$$+W_s^2\left[\frac{1}{2\rho_8}\left(\frac{1}{A_8^2}-\frac{1}{\bar{A}_8^2}\right)+\frac{1}{\rho_8 A_8 A_m}-\frac{1}{\rho_8 A_8^2}-\frac{K_8}{2\rho_8 A_8^2}\right]+W_d^2\left[\frac{1}{2\rho_{13}A_{13}A_m}\right]$$

$$+g_o\left[\bar{\rho}_1(\bar{Z}_1-Z_1)+\bar{\rho}_2(Z_1-Z_2)+\bar{\rho}_4(Z_2-Z_4)+\bar{\rho}_5(Z_4-Z_5)\right.$$

$$+\bar{\rho}_6(Z_5-\bar{Z}_6)+\bar{\rho}_6(\bar{Z}_6-Z_6)+\bar{\rho}_7(Z_6-\bar{Z}_7)+\bar{\rho}_7(\bar{Z}_7-Z_7)$$

$$\left.+\bar{\rho}_8(Z_7-Z_8)+\bar{\rho}_9(Z_8-Z_9)+\bar{\rho}_1(Z_9-\bar{Z}_1)\right]=0$$

Developing the momentum relationships for the jet pump recirculation loop involves the recirculation pump curves. The steady-state operating levels of the recirculation pump for the specific cases analyzed here all fall within a fairly narrow range of the homologous pump curve expressing the pump differential head as a function of flow and speed. Using a linear least squares fit through the three data points describing this portion of the curve results in the expression:

$$\Delta P_{pump} = \frac{g_o}{144 g_c}\left[\frac{m\beta H_r W_d \alpha}{V_r} + \frac{b\beta^2 H_r W_d^2}{V_r^2 \rho_f}\right]$$

The complete derivation of Equation (III-9) and the definitions of the terms are included in the appendices.

The recirculation loop momentum relationship can now be developed, using Equations (III-2) and (III-3) for the jet pump junctions, and Equation (III-1) along with the recirculation pump differential head approximation. This yields the following relationship containing the suction and drive flows, and the normalized pump speed (α):

$$W_s^2\left[\frac{1}{2\rho_8}\left(\frac{1}{A_8^2}-\frac{1}{\bar{A}_8^2}\right)-\frac{1}{\rho_8 A_8^2}-\frac{K_8}{2\rho_8 A_8^2}\right] + W_d^2\left[\frac{1}{2\rho_{11}}\left(\frac{1}{\bar{A}_8^2}-\frac{1}{\bar{A}_{10}^2}\right)\right.$$

$$+\frac{1}{2\rho_{12}}\left(\frac{1}{\bar{A}_{10}^2}-\frac{1}{\bar{A}_{11}^2}\right)-\frac{1}{2\rho_{13}}\left(\frac{1}{\bar{A}_{11}^2}-\frac{1}{\bar{A}_{13}^2}\right)+\frac{1}{\bar{\rho}_{11}\bar{A}_{11}^2}+\frac{2f_{10}l_{10}\phi_{10}}{D_{h10}\bar{\rho}_{10}\bar{A}_{10}^2}$$

$$\left.+\frac{2f_{11}l_{11}\phi_{11}}{D_{h11}\bar{\rho}_{11}\bar{A}_{11}^2}+\frac{K_{11}}{2\rho_{11}A_{11}^2}+\frac{K_{12}}{2\rho_{12}A_{12}^2}+\frac{K_{13}}{2\rho_{13}A_{13}^2}-\frac{g_o\beta^2 H_r b}{V_r^2\bar{\rho}_{10}}\right]$$

$$+g_o\left[\bar{\rho}_8(\bar{Z}_8-Z_8)+\bar{\rho}_9(Z_8-\bar{Z}_9)-\bar{\rho}_8(\bar{Z}_8-Z_{11})-\bar{\rho}_{10}(Z_{11}-Z_{12})\right.$$

$$\left.-\bar{\rho}_{11}(Z_{12}-Z_{13})-\bar{\rho}_9(Z_{13}-\bar{Z}_9)\right] = \frac{g_o\beta H_r m W_d \alpha}{V_r}$$

The three mass balance equations (III-4, 5, 6) and the three pressure balance equations for the closed loops (III-7, 8, 10) constitute a set of six equations in the flow rates W_t, W_c, W_b, W_p, W_s, W_d and W_r as well as the normalized pump speed (α). Therefore, if the steam flow rate is assumed to be known, all of the

other flow rates can be determined as functions of α . In particular, it is then possible to obtain the total flow as a function of α .

The assumption that the steam flow is known independently is justified by the fact that it is primarily a function of the power level. On the other hand, since the flow map (Figure 3) shows that the total flow is very little affected by the power level. This means in turn that the amount of steam flow also has a small effect on the total flow.

In order to facilitate further treatment of the six governing equations, simplifying terminology is introduced for those expressions which are considered constants. Because the equations are quadratic in the flow rates, it appears most convenient to assume a certain total flow (W_t) and solve for all the other flow rates and the pump speed as shown below:

$$\Theta_1 = \left[\frac{1}{2\rho_{10}}\left(\frac{1}{\bar{A}_1^2} - \frac{1}{\bar{A}_3^2}\right) + \frac{1}{2\rho_3}\left(\frac{1}{\bar{A}_3^2} - \frac{1}{\bar{A}_4^2}\right) + \frac{2f_3 l_3 \phi_3}{D_{h_3}\bar{\rho}_3\bar{A}_3^2} + \frac{K_{10}}{2\rho_{10}A_{10}^2} + \frac{K_3}{2\rho_3 A_3^2}\right]$$

$$\Theta_2 = \left[\frac{1}{2\rho_1}\left(\frac{1}{\bar{A}_1^2} - \frac{1}{\bar{A}_2^2}\right) + \frac{1}{2\rho_2}\left(\frac{1}{\bar{A}_2^2} - \frac{1}{\bar{A}_3^2}\right) + \frac{2f_2 l_2 \phi_2}{D_{h_2}\bar{\rho}_2\bar{A}_2^2} + \frac{K_1}{2\rho_1 A_1^2} + \frac{K_2}{2\rho_2 A_2^2}\right]$$

$$\Theta_3 = \left[g_0\left[\bar{\rho}_2(Z_1 - Z_2) - \bar{\rho}_3(Z_{10} - Z_3)\right]\right]$$

Equation (III-7) is reduced to

$$\Theta_1 W_b^2 - \Theta_2 W_c^2 + \Theta_3 = 0$$

and substituting for the core flow by Equation (III-5) gives

$$\Theta_1 W_b^2 - \Theta_2 (W_t^2 - 2W_t W_b + W_b^2) + \Theta_3 = 0$$

Grouping terms in powers of W_b results in

$$(\Theta_1 - \Theta_2) W_b^2 - (2\Theta_2 W_t) W_b + (\Theta_3 - \Theta_2 W_t^2) = 0$$

This equation can now be solved for the bypass flow rate as a function of the total flow rate giving

$$W_b = \frac{(2\Theta_2 W_t) \pm \sqrt{(2\Theta_2 W_t)^2 - 4(\Theta_1 - \Theta_2)(\Theta_3 - \Theta_2 W_t^2)}}{2(\Theta_1 - \Theta_2)}$$

Assuming the total flow rate and the parameters in Θ_1, Θ_2, and Θ_3 are known, the bypass flow rate, and consequently by Equation (III-5), the core flow rate, can be determined as functions of W_t. The "+" sign applies in Equation (III-11) as was verified by comparison of a sample case with results obtained from the RETRAN model.

The vessel loop Equation (III-8) is a function of several flow rates. Assuming a known core thermal power level and therefore the steam flow, the recirculation flow is determined by Equation (III-6) and the previously assumed total flow. Coupled with the previous development for the core loop, the unknown flows in Equation (III-8)

are the suction and drive flows. Substituting as done previously,

$$\Theta_4 = \left[\frac{1}{2\rho_m}\left(\frac{1}{A_m^2} - \frac{1}{\bar{A}_9^2}\right) - \frac{1}{2\rho_4}\left(\frac{1}{\bar{A}_4^2} - \frac{1}{\bar{A}_5^2}\right) - \frac{1}{2\rho_5}\left(\frac{1}{\bar{A}_5^2} - \frac{1}{\bar{A}_6^2}\right) - \frac{1}{2\rho_9}\left(\frac{1}{\bar{A}_9^2} - \frac{1}{\bar{A}_1^2}\right)\right.$$

$$+ \frac{1}{\bar{\rho}_9 \bar{A}_9^2} - \frac{1}{\rho_m A_m^2} - \frac{2f_1 l_1 \phi_1}{D_{h_1} \bar{\rho}_1 \bar{A}_1^2} - \frac{2f_4 l_4 \phi_4}{D_{h_4} \bar{\rho}_4 \bar{A}_4^2} - \frac{2f_5 l_5 \phi_5}{D_{h_5} \bar{\rho}_5 \bar{A}_5^2} - \frac{2f_6 l_6 \phi_6}{D_{h_6} \bar{\rho}_6 \bar{A}_6^2}$$

$$\left. - \frac{2f_8 l_8 \phi_8}{D_{h_8} \bar{\rho}_8 \bar{A}_8^2} - \frac{2f_9 l_9 \phi_9}{D_{h_9} \bar{\rho}_9 \bar{A}_9^2} - \frac{K_4}{2\rho_4 A_4^2} - \frac{K_5}{2\rho_5 A_5^2} - \frac{K_9}{2\rho_9 A_9^2}\right]$$

$$\Theta_5 = \left[\frac{1}{2\rho_1}\left(\frac{1}{\bar{A}_1^2} - \frac{1}{\bar{A}_2^2}\right) + \frac{1}{2\rho_2}\left(\frac{1}{\bar{A}_2^2} - \frac{1}{\bar{A}_4^2}\right) + \frac{2f_2 l_2 \phi_2}{D_{h_2} \bar{\rho}_2 \bar{A}_2^2} + \frac{K_1}{2\rho_1 A_1^2} + \frac{K_2}{2\rho_2 A_2^2}\right]$$

$$\Theta_6 = \left[\frac{1}{2\rho_6}\left(\frac{1}{\bar{A}_6^2} - \frac{1}{\bar{A}_7^2}\right) + \frac{1}{2\rho_7}\left(\frac{1}{\bar{A}_7^2} - \frac{1}{\bar{A}_8^2}\right) + \frac{2f_7 l_7 \phi_7}{D_{h_7} \bar{\rho}_7 \bar{A}_7^2} + \frac{K_6}{2\rho_6 A_6^2} + \frac{K_7}{2\rho_7 A_7^2}\right]$$

$$\Theta_7 = \left[\frac{1}{2\rho_8}\left(\frac{1}{A_8^2} - \frac{1}{\bar{A}_8^2}\right) + \frac{1}{\rho_8 A_8 A_m} - \frac{1}{\rho_8 A_8^2} - \frac{K_8}{2\rho_8 A_8^2}\right]$$

$$\Theta_8 = \left[\frac{1}{2\rho_{13} A_{13} A_m}\right]$$

$$\Theta_9 = \left[g_0\left[\bar{\rho}_1(\bar{Z}_1 - Z_1) + \bar{\rho}_2(Z_1 - Z_2) + \bar{\rho}_4(Z_2 - Z_4) + \bar{\rho}_5(Z_4 - Z_5)\right.\right.$$

$$+ \bar{\rho}_6(Z_5 - \bar{Z}_6) + \bar{\rho}_6(\bar{Z}_6 - Z_6) + \bar{\rho}_7(Z_6 - \bar{Z}_7) + \bar{\rho}_7(\bar{Z}_7 - Z_7)$$

$$\left.\left. + \bar{\rho}_8(Z_7 - Z_8) + \bar{\rho}_8(Z_8 - Z_9) + \bar{\rho}_1(Z_9 - \bar{Z}_1)\right]\right]$$

reduces Equation (III-8) to

$$\theta_4 W_t^2 - \theta_5 W_c^2 - \theta_6 W_r^2 + \theta_7 W_s^2 + \theta_8 W_d^2 + \theta_9 = 0$$

Replacing the drive flow term using Equation (III-4) and rearranging gives

$$(\theta_7+\theta_8)W_s^2 - (2\theta_8 W_t)W_s + [(\theta_4+\theta_8)W_t^2 - \theta_5 W_c^2 - \theta_6 W_r^2 + \theta_9] = 0$$

This also has a quadratic solution. For the suction flow rate, the solution is

$$W_s = \frac{2\theta_8 W_t \pm \sqrt{(2\theta_8 W_t)^2 - 4(\theta_7+\theta_8)[(\theta_4+\theta_8)W_t^2 - \theta_5 W_c^2 - \theta_6 W_r^2 + \theta_9]}}{2(\theta_7+\theta_8)}$$

Thus, Equations (III-4, 5, 6, 11 and 12) uniquely determine all flow rates: W_t (known), W_p (known), W_c, W_b, W_s, W_d, and W_r.

The pump speed can now be determined from Equation (III-10). For this purpose, define

$$\theta_{10} = \left[\frac{1}{2\rho_8}\left(\frac{1}{A_8^2} - \frac{1}{\bar{A}_8^2}\right) - \frac{1}{\rho_8 A_8^2} - \frac{K_8}{2\rho_8 A_8^2}\right]$$

$$\theta_{11} = \left[\frac{1}{2\rho_{11}}\left(\frac{1}{\bar{A}_8^2} - \frac{1}{\bar{A}_{10}^2}\right) + \frac{1}{2\rho_{12}}\left(\frac{1}{\bar{A}_{10}^2} - \frac{1}{\bar{A}_{11}^2}\right) - \frac{1}{2\rho_{13}}\left(\frac{1}{\bar{A}_{11}^2} - \frac{1}{\bar{A}_{13}^2}\right) + \frac{1}{\bar{\rho}_{11}\bar{A}_{11}^2} + \frac{K_{11}}{2\rho_{11}A_{11}^2}\right.$$

$$\left. + \frac{K_{12}}{2\rho_{12}A_{12}^2} + \frac{K_{13}}{2\rho_{13}A_{13}^2} + \frac{2f_{10}\ell_{10}\phi_{10}}{D_{h_{10}}\bar{\rho}_{10}\bar{A}_{10}^2} + \frac{2f_{11}\ell_{11}\phi_{11}}{D_{h_{11}}\bar{\rho}_{11}\bar{A}_{11}^2} - \frac{g_0\beta^2 H_r b}{V_r^2\bar{\rho}_{10}}\right]$$

$$\Theta_{12} = \left[g_o \left[\bar{\rho}_8 (\bar{Z}_8 - Z_8) + \bar{\rho}_9 (Z_8 - \bar{Z}_9) - \bar{\rho}_8 (\bar{Z}_8 - Z_{11}) - \bar{\rho}_{10} (Z_{11} - Z_{12}) \right. \right.$$

$$\left. \left. - \bar{\rho}_{11} (Z_{12} - Z_{13}) - \bar{\rho}_9 (Z_{13} - \bar{Z}_9) \right] \right]$$

$$\Theta_{13} = \frac{g_o \beta H_r m}{V_r}$$

This reduces Equation (III-10) to

$$\Theta_{10} W_s^2 + \Theta_{11} W_d^2 + \Theta_{12} = \Theta_{13} W_d \alpha$$

and solving this equation for α yields

$$\alpha = \frac{\Theta_{10} W_s^2 + \Theta_{11} W_d^2 + \Theta_{12}}{\Theta_{13} W_d}$$

The six equations (III-4, 5, 6, 11, 12, 13) describe the relationships between the seven major flow parameters and the normalized recirculation pump speed for the specification of two of the flow parameters; the total or core recirculation flow, and the steam flow or thermal power level. These relationships are based on the physical characteristics of the flow system, and the assumption that fluid state variables and values for the friction factors are known. This will be the case when a RETRAN steady-state self initialization has been completed for the conditions which have been chosen to serve as a reference case for all other steady-state conditions, as is discussed in the next section.

C. Approximations and Final Solution

The three momentum relationships (Equations III-11, 12, 13) developed in the previous section contain several other quantities which are functions of the state of the system. These are the junction and volume densities, and the single and two-phase friction factors. The densities are fluid state variables, and are determined by the system pressures and enthalpies. The friction factors are determined using the fluid variables and system parameters by means of empirical formulations. The relative changes of these variables have an effect on the pressure drops, and in order to accurately predict the steady-state flows and pump speed, these changes in density and friction terms must be taken into consideration. This process would require bringing in the energy balance equation for determining enthalpies. Also, it would be necessary to rely on iterative techniques for generating the correct mass flow rates since the resulting equations are highly nonlinear; essentially an extensive computing process similar to the steady-state self initialization option in RETRAN.

In order to satisfy goals of keeping the final solution simple so as to not require a complex computer solution, the densities and friction factors are assumed to remain approximately constant. This appears justified since the dominant terms in the momentum equations are the flow rates. The variations of the density and friction factor changes are examined by using the results from the RETRAN simulation cases. They are tabulated in Tables 4 and 5 of Chapter IV, and are seen to be quite small.

Using the above approximations, the "θ" terms in the momentum relationships can be considered as constants. They are obtained using the densities from the 100% power, 100% recirculation flow reference case generated by the RETRAN steady-state self initialization. The friction factors are calculated by hand, also based on the reference case data. The results of these calculations are presented in Appendix C.

The final relationships between the flow rates and pump speed can now be evaluated, with the two flow rates required as input, total flow (W_t) and steam flow (W_p), determined from the BWR power-flow map. The remaining flow parameters and pump speed are calculated using the following procedure:

1. $$W_b = \frac{(2\theta_2 W_t) + \sqrt{(2\theta_2 W_t)^2 - 4(\theta_1 - \theta_2)(\theta_3 - \theta_2 W_t^2)}}{2(\theta_1 - \theta_2)}$$

2. $$W_c = W_t - W_b$$
   $$W_r = W_t - W_p$$

3. $$W_s = \frac{(2\theta_8 W_t) - \sqrt{(2\theta_8 W_t)^2 - 4(\theta_7 + \theta_8)[(\theta_4 + \theta_8)W_t^2 - \theta_5 W_c^2 - \theta_6 W_r^2 + \theta_9]}}{2(\theta_7 + \theta_8)}$$

4. $$W_d = W_t - W_s$$

5. $$\alpha = \frac{\theta_{10} W_s^2 + \theta_{11} W_d^2 + \theta_{12}}{\theta_{13} W_d}$$

IV. RESULTS AND COMPARISONS

The steady-state flow and pump speed predictions from the simplified model developed in Chapter III are presented in Table 1. The corresponding points on the power-flow map expressing the steam and total flows for each case are shown in Figure 8. Case 1 is for reference conditions and was used to determine the correct signs for the quadratic solutions of the flow relationships. Each case represents an equilibrium state as determined using the RETRAN code by modeling a reduction in pump speed and/or insertion of control rods. Cases 1 through 5 represent the rated flow control line resulting from pump speed reduction only. Similarly, Cases 6 through 10 and 11 through 15 also form flow control lines for two different rod patterns. The near vertical displacement between lines due to the introduction of negative reactivity is in increments of $1.50.

A complete list of flow and pump speed results from the RETRAN runs is presented in Table 2. It should be noted that these figures were obtained by RETRAN simulation over a period of 150 seconds, and although they are relatively accurate, minor changes in the system variables are expected since the systems were not quite at steady-state equilibrium. Better agreement may have resulted if the transients had been run out longer to get closer approximations to asymptotic equilibrium states.

Table 3 gives a comparison between the two sets of results for core and drive flows, and pump speeds. The reference case comparison shows minor discrepancies between the results from the simplified model and the RETRAN calculations. This is attributable to

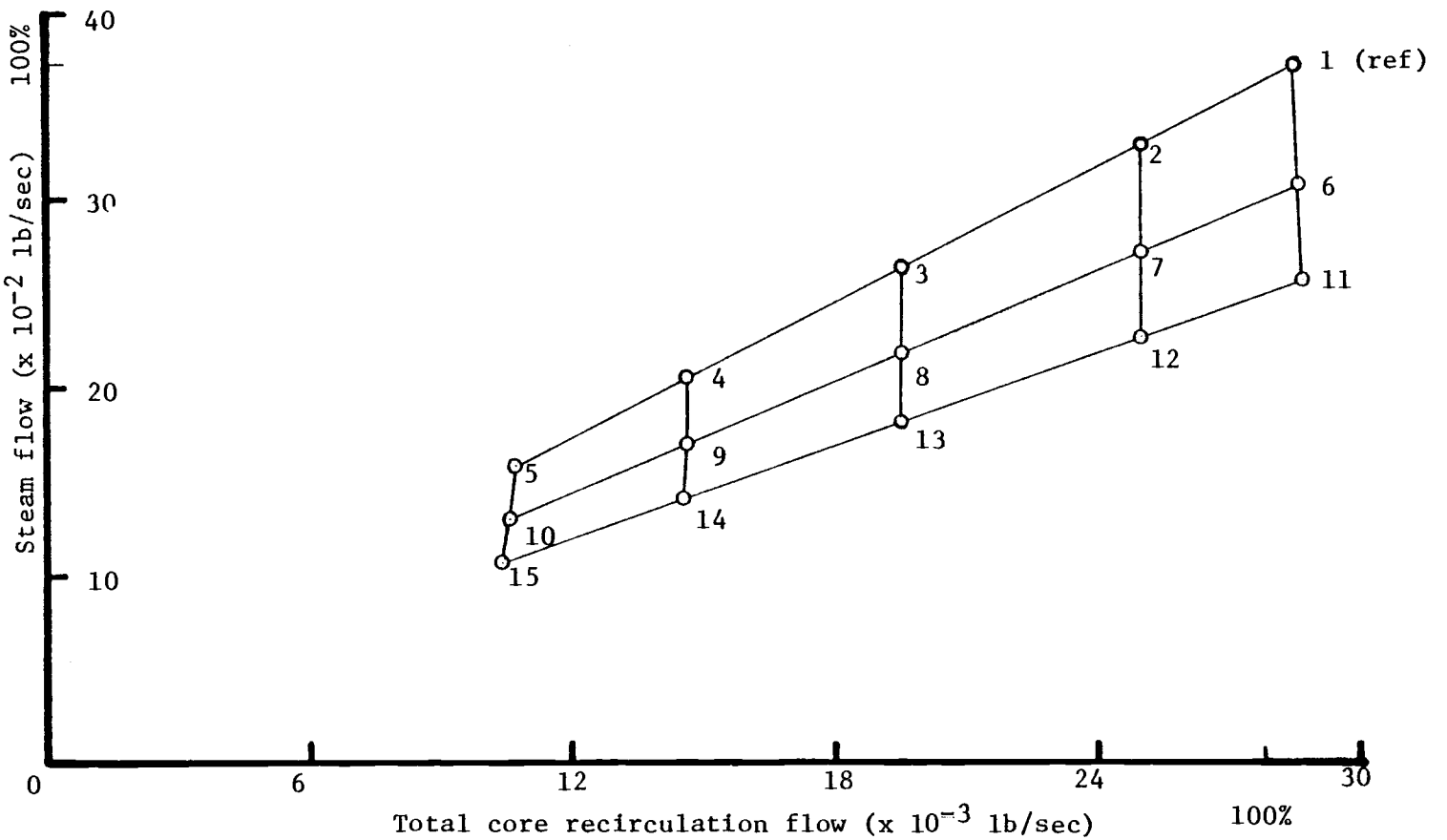

Figure 8. BWR Power-Flow Map from RETRAN Results.

Table 1. Results of the Simplified Model

Case No.	Flow Rates (lb/sec) Total* Flow	Steam* Flow	Core Flow	Bypass Flow	Recirculation Flow	Suction Flow	Drive Flow	Normalized Pump Speed
1	28472.2	3716.8	26012.4	2459.8	24755.4	19455.7	9016.5	0.9219
2	24987.1	3302.7	22865.9	2121.2	21684.4	17188.7	7798.4	0.7951
3	19551.9	2654.5	17975.4	1576.5	16897.4	13703.6	5848.3	0.5910
4	14617.8	2063.5	13576.0	1041.8	12554.3	10659.3	3958.5	0.3902
5	10717.3	1596.8	10193.5	523.8	9120.5	8523.9	2193.4	0.1918
6	28581.5	3095.0	26111.1	2470.4	25486.5	19523.3	9058.2	0.9263
7	25062.7	2748.4	22934.0	2128.7	22314.3	17234.3	7828.4	0.7983
8	19571.6	2204.3	17993.1	1578.5	17367.3	13713.2	5858.4	0.5921
9	14563.8	1702.5	13528.3	1035.5	12861.3	10624.7	3939.1	0.3881
10	10580.5	1304.8	10079.4	501.1	9272.1	8458.6	2121.9	0.1831
11	28650.8	2576.7	26173.8	2477.0	26074.1	19565.3	9085.5	0.9291
12	25096.3	2284.8	22964.4	2131.9	22811.5	17253.2	7843.1	0.7999
13	19551.1	1824.3	17974.7	1576.4	17726.8	13697.8	5853.3	0.5916
14	14472.7	1397.4	13447.8	1024.9	13075.3	10568.6	3904.1	0.3844
15	10401.5	1059.1	9931.2	470.3	9342.4	8376.9	2024.6	0.1712

*from RETRAN results

Table 2. Results of the RETRAN Calculations

Case No.	Flow Rates (lb/sec)							Normalized Pump Speed
	Total Flow	Steam Flow	Core Flow	Bypass Flow	Recirculation Flow	Suction Flow	Drive Flow	
1	28472.2	3716.8	26011.8	2460.4	24755.4	19453.1	9019.1	0.9247
2	24987.1	3303.5	22851.9	2135.2	21683.6	17162.8	7824.3	0.80
3	19551.9	2657.1	17936.5	1615.4	16894.8	13638.3	5913.6	0.60
4	14617.8	2068.9	13523.7	1094.1	12548.9	10577.4	4040.4	0.40
5	10717.3	1607.5	10128.6	588.7	9109.8	8451.8	2265.5	0.20
6	28581.5	3095.0	26168.1	2413.4	25486.5	19586.7	8994.8	0.9247
7	25062.7	2748.4	22971.0	2091.7	22314.3	17261.8	7800.9	0.80
8	19571.6	2204.3	17995.7	1575.9	17367.3	13678.7	5892.9	0.60
9	14563.8	1702.5	13505.2	1058.6	12861.3	10544.0	4019.8	0.40
10	10580.5	1308.4	10026.8	553.7	9272.1	8334.9	2245.6	0.20
11	28650.8	2576.7	26279.5	2371.3	26074.1	19675.0	8975.8	0.9247
12	25096.3	2284.8	23043.3	2053.0	22811.5	17314.0	7782.3	0.80
13	19551.1	1824.3	18008.6	1542.5	17726.8	13677.6	5873.5	0.60
14	14472.7	1397.4	13442.3	1030.4	13075.3	10471.2	4001.5	0.40
15	10401.5	1059.1	9875.1	526.4	9342.4	8176.5	2225.0	0.20

Table 3. Comparison of Results

Case No.	Core Flow			Drive Flow			Normalized Pump Speed		
	Approx.	RETRAN		Approx.	RETRAN		Approx.	RETRAN	
1	26012.4	26011.8	-0.6	9016.5	9019.1	2.6	0.9219	0.9247	0.0028
2	22865.9	22851.9	-14.0	7798.4	7824.3	25.9	0.7951	0.80	0.0049
3	17975.4	17936.5	-38.9	5848.3	5913.6	65.3	0.5910	0.60	0.0090
4	13576.0	13523.7	-52.3	3958.5	4040.4	81.9	0.3902	0.40	0.0098
5	10193.5	10128.6	-64.9	2193.4	2265.5	72.1	0.1918	0.20	0.0082
6	26111.1	26168.1	57.0	9058.2	8994.8	-63.4	0.9263	0.9247	-0.0016
7	22934.0	22971.0	37.0	7828.4	7800.9	-27.5	0.7983	0.80	0.0017
8	17993.1	17995.7	2.6	5858.4	5892.9	34.5	0.5921	0.60	0.0079
9	13528.3	13505.2	-23.1	3939.1	4019.8	80.7	0.3881	0.40	0.0119
10	10079.4	10026.8	-52.6	2121.9	2245.6	123.7	0.1831	0.20	0.0169
11	26173.8	26279.5	105.7	9085.5	8975.8	-109.7	0.9241	0.9247	-0.0044
12	22964.4	23043.3	78.9	7843.1	7782.3	-60.8	0.7499	0.80	0.0001
13	17974.7	18808.6	33.9	5853.3	5873.5	20.2	0.5916	0.60	0.0084
14	13447.8	13442.3	-5.5	3904.1	4001.5	97.4	0.3844	0.40	0.0156
15	9931.2	9875.1	-56.1	2024.6	2225.0	200.4	0.1712	0.20	0.0288

round-off errors in the information taken from the RETRAN reference case, in hand calculations of the friction factors from the empirical formulations, and to the approximation used for the recirculation pump performance curve. In any case, the reference case results from the simplified model are in good agreement, showing nominal error in the flow and pump speed comparisons (See Figures 9 and 10). The flow rate predictions are seen to have errors of no more than 2.25% from their reference case values. A comparison of pump speed results indicates errors no more than 3.15% of the reference case pump speed. The largest errors were found for conditions which occupy the lower left corner of the flow map, i.e., which are furthest away from the reference case.

The errors in the flow and pump speed predictions result from the change in fluid density and friction losses between steady-state levels, and from the pump approximation. The core flow and drive flow results indicate that the relative changes in densities and friction factors tend to offset each other under certain conditions. Tables 4 and 5 present the densities and friction factors for selected volumes and junctions for different steady-state cases as determined by RETRAN. These results are primarily concerned with the volumes which contain two-phase mixtures. The densities in the volumes containing subcooled water change relatively little, and the friction factors are primarily functions of the fluid flow rate, i.e., a decrease in the flow rate results in an increase in the fanning friction factor for turbulent flow conditions.

Table 4. Selected Volume and Junction Densities from the RETRAN Test Cases

Case No.	Volume Density (lb/ft^3) Volume 2 (Core)	Volume 4 (Upper Plenum)	Volume 5 (Stand Pipes)	Volume 6 (Stm.Sep.)	Junction Density (lb/ft^3) Junction 2 (Vol 2-Vol 4)	Junction 4 (Vol 4-Vol 5)	Junction 5 (Vol 5-Vol 6)
1	28.5642	13.2442	13.1021	23.7473	12.3364	13.2287	13.0896
2	28.3785	13.0541	12.9407	23.9116	12.1700	13.0392	12.9299
3	28.0782	12.6993	12.6255	24.3353	11.8516	12.6886	12.6160
4	27.7924	12.2626	12.2169	24.8509	11.5198	12.2543	12.2090
5	27.5651	11.7051	11.6769	25.2536	11.1917	11.6988	11.6705
6	29.3066	14.9823	14.8252	29.5958	14.0532	14.9629	14.8103
7	29.6386	14.8001	16.6735	28.5716	13.8647	14.7839	14.6588
8	29.3670	14.4595	14.3757	27.4028	13.5694	14.4462	14.3632
9	29.0931	14.0378	13.9850	26.7391	13.2553	14.0272	13.9744
10	28.8974	13.4619	13.4284	26.4759	12.9278	13.4536	13.4196
11	31.1002	16.8626	16.6840	33.8198	15.8808	16.8405	16.6635
12	30.9501	16.6890	16.5464	31.9254	15.7188	16.6692	16.5279
13	30.6941	16.3670	16.2715	29.5775	15.4403	16.3505	16.2553
14	30.4462	15.9646	15.9032	28.1020	15.1466	15.9512	15.8891
15	30.2667	15.3869	15.3565	27.2476	14.8325	15.3758	15.3342

Table 5. Selected Friction Factors from Some RETRAN Test Cases

Case No.	Friction Factors (f_Φ)							
	Vol. 1	Vol. 2	Vol. 3	Vol. 4	Vol. 5	Vol. 6	Vol. 10	Vol. 11
1	0.00318	0.00799	0.00438	0.02608	0.00793	0.00487	0.00168	0.00187
2	0.00326	0.00838	0.00453	0.02806	0.00839	0.00503	0.00170	0.00191
3	0.00340	0.00914	0.00482	0.03162	0.00997	0.00552	0.00177	0.00198
6	0.00318	0.00754	0.00440	0.02279	0.00707	0.00397	0.00168	0.00137
11	0.00317	0.00704	0.00441	0.01924	0.00632	0.00343	0.00167	0.00186

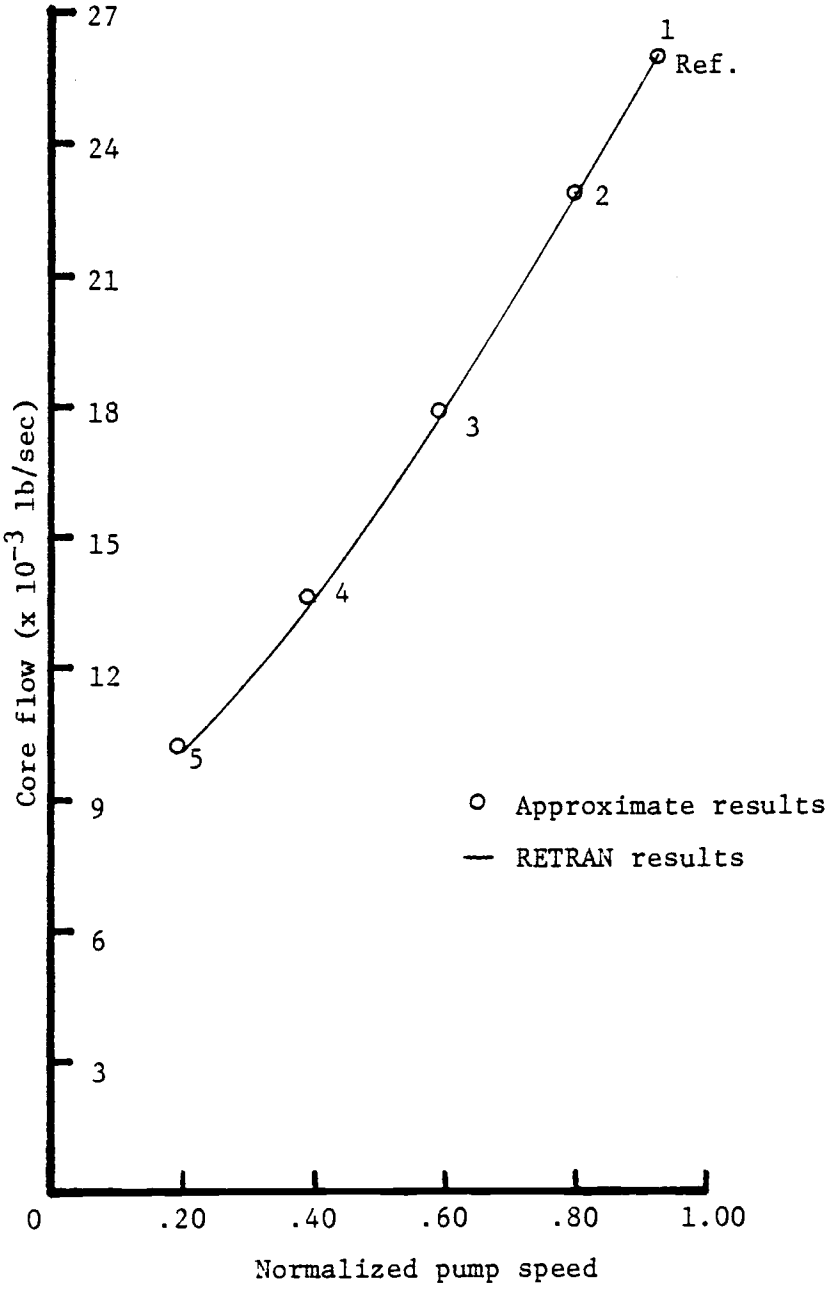

Figure 9. Comparison of Core Flow Rate Predictions for Pump Speed Reduction.

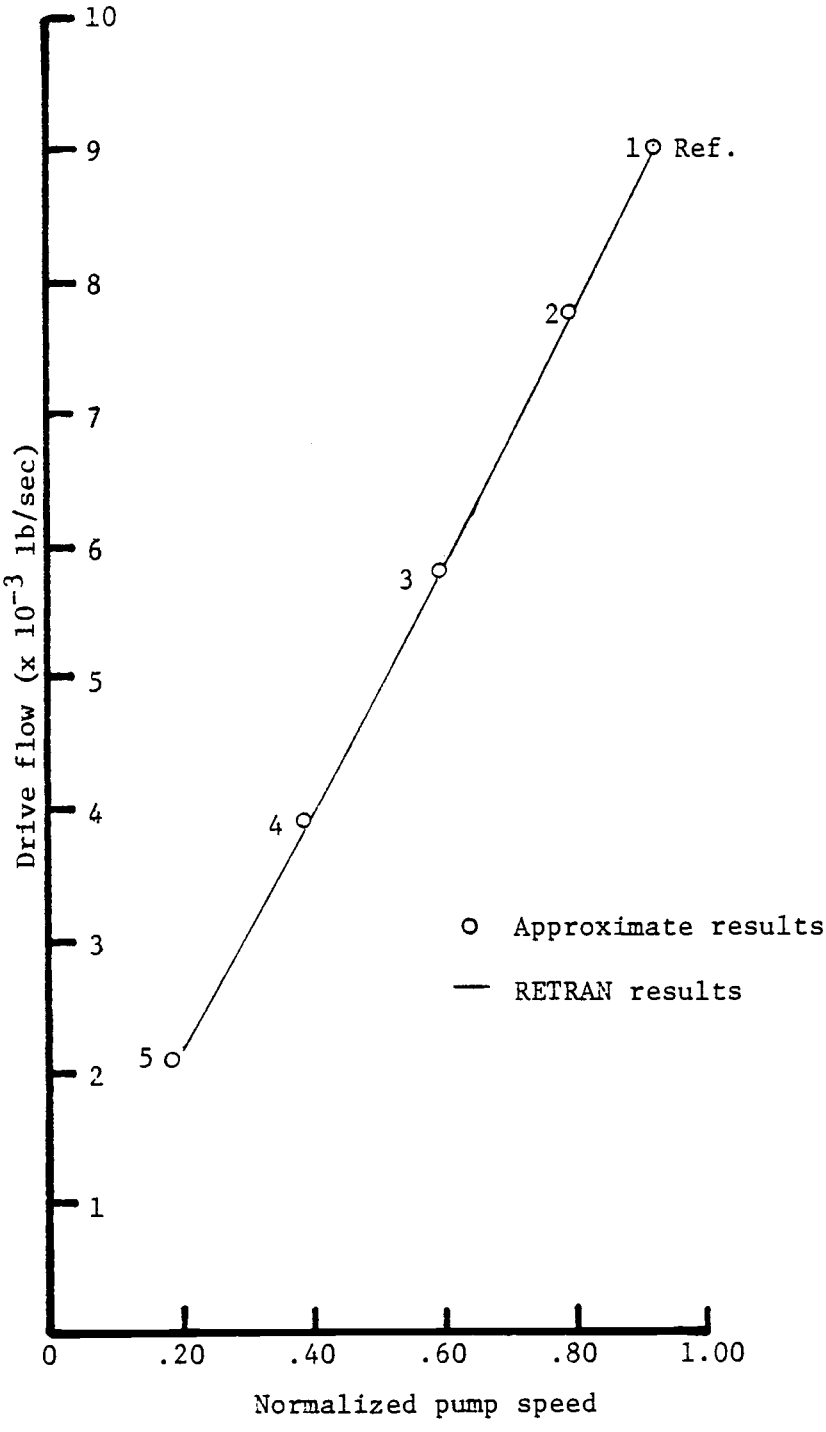

Figure 10. Comparison of Drive Flow Rate Predictions for Pump Speed Reduction.

Perturbation:	Reduce recirculation pump speed
Overall Effects:	Decrease in thermal power level
	Decrease in system flow rates
	Decrease in system pressure
Specific Effects:	Increase in density in steam separator and steam sep. ext.
	Increase in density in subcooled liquid regions (small)
	Decrease in density in two-phase regions
	Increase in friction factors in subcooled liquid regions
	Increase in friction factors in two-phase regions

Flow Prediction Error Trend in the Simplified Model:

Core flow underpredicted - drive flow overpredicted

Figure 11. RETRAN Prediction of the Generalized Behavior of a BWR Due to a Recirculation Pump Speed Reduction.

Perturbation:	Insert control rod(s)
Overall Effects:	Decrease in thermal power level
	Small changes in system flow rates
	Decrease in system pressure
Specific Effects:	Increase in density in steam separator and steam sep. ext.
	Decrease in density in subcooled liquid regions (small)
	Increase in density in two-phase regions
	Decrease in friction factors in subcooled liquid regions (small)
	Decrease in friction factors in two-phase regions

Flow Prediction Error Trend in the Simplified Model:

Core Flow Over Predicted - Drive Flow Underpredicted

Figure 12. RETRAN Prediction of the Generalized Behavior of a BWR Due to an Insertion of Negative Reactivity.

Analysis of the relative changes in the fluid densities and friction factors for the cases studied supports the flow rate results obtained and gives some indication of the sources of error involved when comparing the results from the simplified model to the RETRAN calculations. This information is presented in Figures 11 and 12 for pump speed reduction and control rod insertion, respectively.

The errors associated with the pump speed calculations are attributable to two approximations; the errors involving the drive flow calculation, and thus associated with the aforementioned density and friction factor approximations, and second, the approximation for the pump performance curve. The errors associated with the drive flow predictions are related to the information presented in Figures 11 and 12. The pump approximation is examined in Appendix B.

Figure 13 shows the relationship between the steam flow and the thermal power level. The linear relationship is evident, demonstrating that knowing the power level of the plant, one can find the steam flow rate, and indicating that the power level is essentially independent of the total flow, as is shown by Figure 8, the power-flow map.

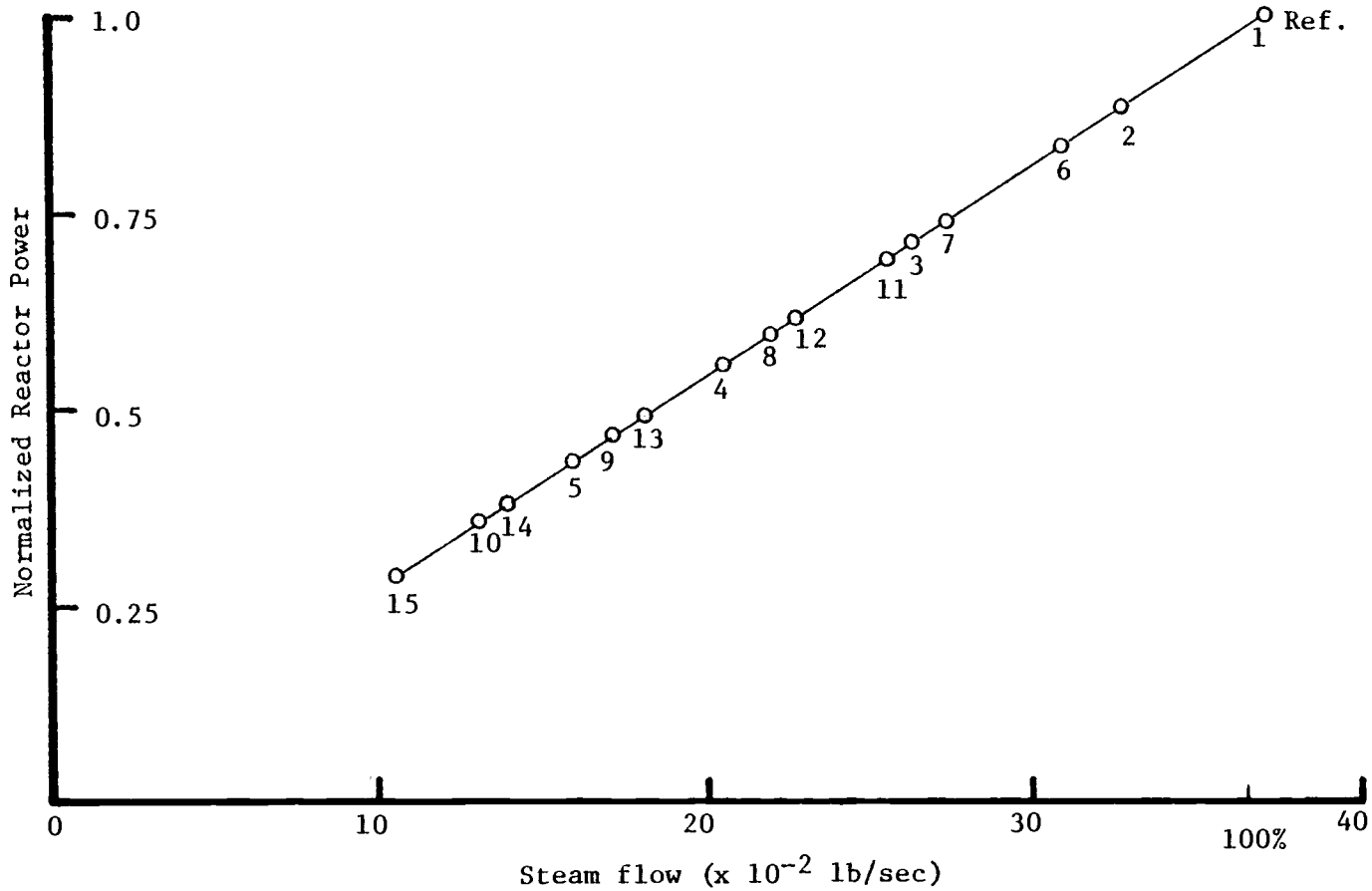

Figure 13. BWR Power vs. Steam Flow from RETRAN Calculations.

V. CONCLUSIONS

Examination of the relative density and friction factor changes in comparing various steady-states obtained by RETRAN reveals the problems associated with using the approximations of constant density and friction factors in the simplified model. These changes can be separately associated with the two control methods used to change the operating level, reduction of pump speed, and insertion of control rods.

As a result of the pump speed reduction, the power level (steam flow rate) is reduced. At the same time there is a reduction in the flow rates (i.e., total flow is reduced, less coolant is flowing through the system), and a decrease in the system pressure. As a result of the flow reductions, the friction factors in subcooled liquid regions increase, as do the friction factors in two-phase flow regions. This second change is attributable to a decrease in the fluid density in the core, for even though there is less steam produced, the core flow drops significantly, resulting in a relative decrease in the density (i.e., higher void fraction) in the core and upper internals. This result also demonstrates the decrease in neutron moderation discussed previously. The average density in the steam separator increases due to the reduction in steam production and subsequent rise in the mixture level. In general, the different relative changes in densities and subsequently the friction factor changes due to both density and flow rate reduction, are responsible for the errors in flow rates determined by using the simplified model.

Inserting control rods results in a reduction of power, but there is relatively little change in the flow rates as is shown in the power-flow map (Figure 8). However, the density in compressible flow regions is increased. This effect is easily understood by examining the reduction in power level corresponding to reduced steam production while maintaining total flow. More of the coolant remains as a saturated liquid and the increased density effects a large decrease in the two-phase friction factors, hence the flow prediction errors should tend to vary in the opposite direction as those determined for the pump speed reduction cases. This is verified in Table 3, where Cases 1 through 5 show tendencies to underpredict the core flow and overpredict the drive flow rate, and Cases 1, 6, and 11 indicate just the opposite.

The two major sources of error are; (1) relative density changes in two-phase regions, which in turn is related to friction factor variation, and (2) changes in friction factors for liquid phase regions due to changing flow rates, both of which are neglected in the simplified model. However, the two control mechanisms have opposite effects on the density, indicating that using both pump speed reduction and control rod insertion should tend to create an offsetting effect to some extent. This logic is supported by the results in Table 3, where improved accuracy for flow rate predictions is found in Cases 7, 8, 13 and 14.

Errors associated with the pump speed predictions are interdependent on the accuracy of drive flow calculations, and the approximation used to represent pump characteristics. As previously

mentioned, a linear least squares fit over three data points was used to generate the results presented in Chapter IV. Subsequently, another set of tests were conducted using a linear approximation between two data points. The RETRAN calculations are based on linear interpolation between two adjacent points on the homologous pump curves; therefore, the error due to a poor pump approximation is eliminated in the tests for specific cases. This resulted in only nominal improvement in the accuracy of the pump speed predictions for these cases (1, 2, 6, 7, 11, and 12), hence indicating that the majority of the error is a result of inaccuracy in determining the drive flow.

The previous discussion points out the shortcomings of the simplified model. The results in Table 3 indicate that the approximate solution tends to provide better accuracy for pump speed reduction than for insertion of control rods. The reason for this is given in Table 4, where the densities vary more for the control rod insertion cases. Conversely, the friction factor changes in liquid filled volumes are negligible for control rod insertion, since the flow rates undergo little change, thus giving further indication that the errors in flow calculations are primarily due to density changes in two-phase regions.

Based on this analysis, the limitations for predicting the flow rates and pump speeds at various steady-state operating levels using this method (for BWR's) can be summarized in the following manner. Predictions for flows and pump speeds along a flow control line are relatively good, with error increasing in an approximately linear

fashion for increasing deviation from the reference conditions. Predictions for control rod repositioning are somewhat more inaccurate. Using both control mechanisms tends to improve the accuracy of the flow predictions to a limited extent and there appear to be regions of the power-flow map where the densities are approximately constant, and flow predictions are consequently quite accurate.

In conclusion, this method provides good overall results for predicting the major flow parameters and recirculation pump speeds without requiring a complex iterative solution when used within the aforementioned limitations. Since the magnitude of the perturbation has a strong influence on the accuracy it may, in fact, be more efficient to establish several consistent reference states with RETRAN, and use each reference case to develop a corresponding set of data parameters for making predictions in the vicinity of each reference state.

VI. BIBLIOGRAPHY

1. Final Safety Analysis Report, Peach Bottom 2 Atomic Power Station Units 2 and 3, Philadelphia Electric Company.

2. N. H. Larsen. Core Design and Operating Data for Cycles 1 and 2 of Peach Bottom 2. EPRI NP-563, June 1978.

3. L. A. Carmichael and R. O. Niemi. Transient and Stability Tests at Peach Bottom Atomic Power Station Unit 2 at End of Cycle 2. EPRI NP-564, June 1978.

4. K. Hornyik and J. A. Naser. RETRAN Analysis of the Turbine Trip Tests at Peach Bottom Atomic Power Station Unit 2 at the End of Cycle 2. EPRI NP-1076-SR, April 1979.

5. K. V. Moore et al. RETRAN - A Program for One-Dimensional Transient Thermal-Hydraulic Analysis of Complex Fluid Flow Systems. EPRI NP-408, Vols. 1-4, December 1978.

6. N. S. Burrell et al. A RELAP4 Analysis of the GE BWR Blowdown Heat Transfer Two-Loop Test Apparatus Experiments, Tests 4902, 4903, 4904, and 4906. EPRI NP-169, November 1976.

APPENDICES

APPENDIX A

Nomenclature

A_j = junction flow area (ft^2)

$\bar{A}_k$ = volume flow area (ft^2)

b = y intercept for the linear pump approximation (dimensionless)

Dh_k = volume hydraulic diameter (ft)

f_k = fanning friction factor (dimensionless)

g_o = gravitational acceleration = 32.174 (ft/sec^2)

H_r = pump rated head (ft)

K_k = junction form loss coefficient (dimensionless)

l_k = volume flow length (ft)

m = slope for the linear pump approximation (dimensionless)

P_k = thermodynamic pressure at volume center (psi)

R_e = Reynolds number (dimensionless)

V_r = pump rated flow (gpm)

V_j = junction fluid velocity (ft/sec)

W_j = junction flow rate (lb/sec)

$\bar{W}_k$ = volume flow rate (lb/sec)

W_b = core bypass flow rate (lb/sec)

W_c = core flow rate (lb/sec)

W_d = recirculation pump (drive) flow rate (lb/sec)

W_p = steam flow rate (lb/sec)

W_r = recirculation flow rate (lb/sec)

W_s = jet pump suction flow rate (lb/sec)

W_t = total (core recirculation) flow rate (lb/sec)

Z_j = junction elevation (ft)

Z_k = volume elevation at center (ft)

α = normalized pump speed (dimensionless)

β = conversion factor = 448.83 (gal-sec)/(ft^3-min)

ϕ_k = modified Baroczy two-phase friction factor (dimensionless)

ρ_1 = junction density (lb/ft^3)

$\bar{\rho}_k$ = volume density (lb/ft^3)

Subscripts:

j = junction conditions

k = upstream volume conditions

l = downstream volume conditions

j_1 = drive flow junction conditions

j_2 = suction flow junction conditions

m = jet pump mixing section conditions

Terms:

$\frac{\bar{W}_k^2}{\bar{\rho}_k \bar{A}_k^2} - \frac{\bar{W}_l^2}{\bar{\rho}_l \bar{A}_l^2}$ = momentum flux due to density change

$\frac{W_j^2}{2\rho_j}\left(\frac{1}{\bar{A}_k^2} - \frac{1}{\bar{A}_l^2}\right)$ = momentum flux due to area change

$\frac{K_j W_j^2}{2\rho_j A_j^2}$ = junction friction pressure loss due to form drag and area changes

$\frac{f_k l_k \phi_k \bar{W}_k^2}{D_{hk} \bar{\rho}_k \bar{A}_k^2}$ = friction pressure loss within each half-volume

Note: For two-phase conditions, the density is the saturated liquid density, ρ_f

$g_o[\bar{\rho}_K(\bar{Z}_K - Z_j)]$ = gravity pressure differential from volume center to junction

APPENDIX B

Recirculation Pump Analysis

The RETRAN computer code contains a submodule for modeling a centrifugal pump. A complete description of the pump module is presented in Reference 5, and only a brief description is supplied here pertaining to the information required for this thesis.

The pump model requires the input of data in tabular form describing the pump characteristics as related to the pump fluid. The pump is modeled as a volume, and the pump head is added to upstream and downstream junctions in equal portions. The head is obtained from pump characteristic curves which are supplied to the code in their homologous form, i.e., the head ratios (actual/rated) are input as functions of the pump speed and volumetric flow ratios. The torque ratios are also input in the same manner, but are not applicable to this analysis. The characteristic parameters are defined as:

α = speed ratio

h = head ratio

v = flow ratio

Linear interpolation is used to develop continuous relationships.

For this analysis the relation of interest is that relating pump speed, head, and flow. From the RETRAN input:

v/α	h/α^2	α/v	h/v^2
0.4	1.325	0.77	0.405
0.6	1.246	0.87	0.650
0.8	1.150	0.975	0.91483
1.0	1.0	1.0	1.0

H_r = 716.5 ft (rated head)

V_r = 90,400 gpm (rated flow)

N_r = 1668 rpm (rated speed)

The tabulated data is plotted in Figure B1. In order to determine the specific operating region of interest, the RETRAN results for the test cases were used to determine the steady-state operating levels for the pump. These are tabulated in Table B1, and indicate that the curve between the points (α /v = 0.87, h/v^2 = 0.650) and (α /v = 1.0, h/v^2 = 1.0) contains most of the pump performance levels needed for this study, with the 20% pump speed cases outside of this range.

Using a linear least squares fit through the three points of interest:

x	y	x^2	y^2	xy	
0.87	0.650	0.7569	0.4225	0.5655	
0.975	0.91473	0.9506	0.8368	0.8919	
1.0	1.0	1.0	1.0	1.0	
2.845	2.565	2.7075	2.2592	2.4574	TOTALS

$$SS_{xx} = \sum x^2 - \frac{(\sum x)^2}{n} = 0.0095$$

$$SS_{xy} = \sum xy - \frac{(\sum x)(\sum y)}{n} = 0.0251$$

The slope is

$$m = \frac{SSxx}{SSxx} = 2.6420$$

The intercept is

$$b = \bar{y} - m\bar{x} = -1.6506$$

and the linear approximation is

$$y = mx+b$$

From the curves

$$y = \frac{h}{v^2} = \frac{H}{H_r} \cdot \frac{V_r^2}{V^2}$$

Substituting for x and y

$$\frac{H}{H_r} \cdot \frac{V_r^2}{V^2} = \frac{m V_r a}{V} + b$$

and solving for the pump head gives

$$H = \frac{Hr\,Vm\,\alpha}{Vr} + \frac{Hr\,V^2 b}{Vr^2} \qquad (Ft)$$

$$H = \left[\frac{\rho g_o}{144 g_c}\left(\frac{Hr\,Vm\,\alpha}{Vr} + \frac{Hr\,V^2 b}{Vr^2}\right)\right] \qquad (PSI)$$

Using the following to replace the flow term (V),

$$V = \frac{Wd\ (LB/SEC)}{\rho\ (LB/FT^3)} \cdot \frac{\beta\ (GPM)}{(FT^3/SEC)} = \frac{Wd\,\beta}{\rho}\ (GPM)$$

$$\beta = 448.83\ (GPM)/(FT^3/SEC)$$

gives

$$H = \frac{\rho g_o}{144 g_c}\left[\frac{Hr\,Wd\,\beta m\,\alpha}{\rho\,Vr} + \frac{Hr\,Wd^2\beta^2 b}{\rho^2 Vr^2}\right]$$

$$H = \frac{g_o}{144 g_c}\left[\frac{m\,\beta\,Hr\,Wd\,\alpha}{Vr} + \frac{b\,\beta^2 Hr\,Wd^2}{Vr^2\,\rho}\right]$$

and substituting ΔP_{pump} for H gives the final relationship

$$\Delta P_{pump} = \frac{g_c}{144 g_c}\left[\frac{m\beta H_r W_d \alpha}{V_r} + \frac{b\beta^2 H_r W_d^2}{V_r^2 \rho}\right] \quad (PSI)$$

which represents the pump head as a function of the normalized pump speed (α) and the drive flow rate (W_d), and the numerical values of the constants in the above equation are

$m = 2.6420$

$b = -1.6506$

$H_r = 716.5$ (ft)

$V_r = 90.400$ (gpm)

$\beta = 448.83$ (gpm)/(ft^3/sec)

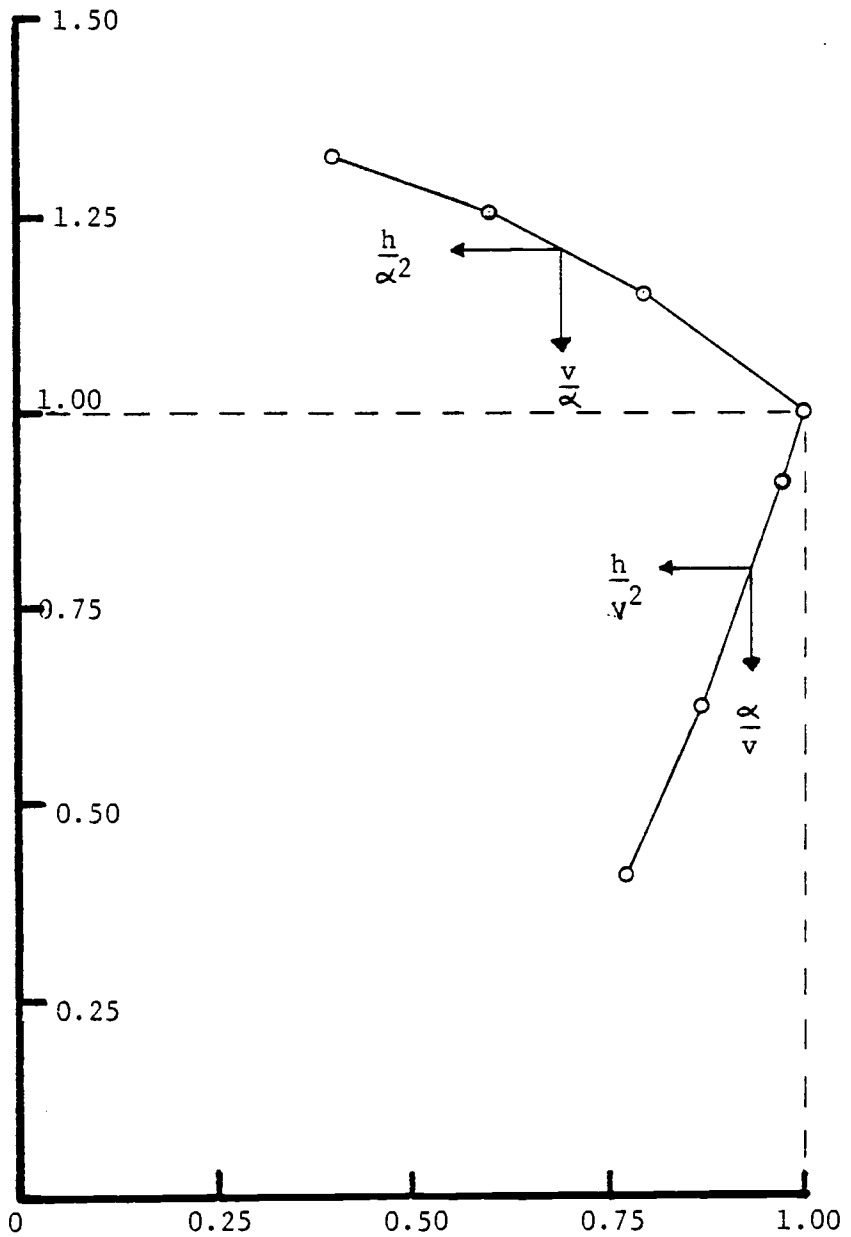

Figure B1. Homologous Pump Head Curve.

Table B1. Pump Performance Data from RETRAN Results

Case No.	Normalized Pump Speed (α)	Volumetric Flow Rate (V)	Normalized Vol. Flow (ν)	$\frac{\alpha}{\nu}$	$\frac{h}{\nu^2}$
1	0.9247	85185.5	0.9423	0.9813	0.9362
2	0.80	73812.7	0.8165	0.9798	0.9311
3	0.60	55685.7	0.6160	0.9740	0.9122
4	0.40	37969.6	0.4200	0.9523	0.8575
5	0.20	21250.8	0.2351	0.8508	0.6030
6	0.9247	85269.3	0.9432	0.9803	0.9328
7	0.80	73884.1	0.8173	0.9788	0.9277
8	0.60	55728.5	0.6165	0.9733	0.9104
9	0.40	37962.5	0.4199	0.9525	0.8580
10	0.20	21173.9	0.2342	0.8539	0.6106
11	0.9247	85322.0	0.9438	0.9797	0.9308
12	0.80	73934.6	0.8179	0.9782	0.9256
13	0.60	55753.0	0.6167	0.9729	0.9094
14	0.40	37948.6	0.4198	0.9529	0.8590
15	0.20	21076.4	0.2331	0.8578	0.6201

APPENDIX C

Derivations and Detailed Analysis

The full development of the simplified model solution is presented here. Included is a complete tabulation of the numerical values for the reference case as applied to the simplified model.

The analysis is based on the steady-state mass and momentum conservation equations. The following momentum equations describe the pressure drops across junctions. For the simply connected volumes,

$$P_\ell - P_K = \frac{1}{144 g_c}\left[\frac{\bar{W}_K^2}{\bar{\rho}_K \bar{A}_K^2} - \frac{\bar{W}_\ell^2}{\bar{\rho}_\ell \bar{A}_\ell^2} - \frac{W_j^2}{2\rho_j}\left(\frac{1}{\bar{A}_K^2} - \frac{1}{\bar{A}_\ell^2}\right)\right.$$

$$-\left(\frac{f_K l_K \phi_K \bar{W}_K^2}{D_{hK} \bar{\rho}_K \bar{A}_K^2} + \frac{f_\ell l_\ell \phi_\ell \bar{W}_\ell^2}{D_{h\ell} \bar{\rho}_\ell \bar{A}_\ell^2}\right) - \frac{K_j W_j^2}{2\rho_j \bar{A}_j^2}$$

$$\left. + g_o\left(\bar{\rho}_K(\bar{Z}_K - Z_j) + \bar{\rho}_\ell(Z_j - \bar{Z}_\ell)\right)\right]$$

For the jet pump drive flow junction,

$$P_\ell - P_{K1} = \frac{1}{144 g_c}\left[\frac{W_{j1}^2}{2\rho_{j1}}\left(\frac{1}{\bar{A}_{K1}^2} - \frac{1}{A_{j1}^2}\right) + \frac{W_m^2}{2\rho_m}\left(\frac{1}{A_m^2} - \frac{1}{\bar{A}_\ell^2}\right)\right.$$

$$+ \frac{W_{j1}V_{j1} + W_{j2}V_{j2} - W_m V_m}{A_m} - \left(\frac{f_{K1} l_{K1} \phi_{K1} \bar{W}_{K1}^2}{D_{hK1} \bar{\rho}_{K1} \bar{A}_{K1}^2} + \frac{f_\ell l_\ell \phi_\ell \bar{W}_\ell^2}{D_{h\ell} \bar{\rho}_\ell \bar{A}_\ell^2}\right)$$

$$\left. - \frac{K_{j1} W_{j1}^2}{2\rho_{j1} A_{j1}^2} + g_o\left(\bar{\rho}_{K1}(\bar{Z}_{K1} - Z_{j1}) + \bar{\rho}_\ell(Z_{j1} - \bar{Z}_\ell)\right)\right]$$

and for the jet pump suction flow junction,

$$P_\ell - P_{K2} = \frac{1}{144 g_c}\left[\frac{\overline{W}_{K2}^2}{\overline{\rho}_{K2}\overline{A}_{K2}^2} - \frac{\overline{W}_{j2}^2}{\rho_{j2}\overline{A}_{j2}^2} + \frac{W_{j2}^2}{2\rho_{j2}}\left(\frac{1}{A_{j2}^2} - \frac{1}{\overline{A}_{K2}^2}\right) + \frac{W_m^2}{2\rho_m}\left(\frac{1}{A_m^2} - \frac{1}{\overline{A}_\ell^2}\right)\right.$$

$$+ \frac{W_{j1}V_{j1} + W_{j2}V_{j2} - W_m V_m}{A_m} - \left(\frac{f_{K2}\ell_{K2}\phi_{K2}\overline{W}_{K2}^2}{Dh_{K2}\overline{\rho}_{K2}\overline{A}_{K2}^2} + \frac{f_\ell \ell_\ell \phi_\ell \overline{W}_\ell^2}{Dh_\ell \overline{\rho}_\ell \overline{A}_\ell^2}\right)$$

$$\left. - \frac{K_{j2}W_{j2}^2}{2\rho_{j2}A_{j2}^2} + g_o\left(\overline{\rho}_{K2}(\overline{Z}_{K2} - Z_{j2}) + \overline{\rho}_\ell(Z_{j2} - Z_\ell)\right)\right]$$

Simplifying the momentum equations in order to facilitate development of the close loop formulations results in the following general expression for the momentum equations,

$$\Delta P_j = \frac{1}{144 g_c}\left[\Delta P(s)_j - \Delta P(f)_j + \Delta P(z)_j\right]$$

where

$$\Delta P_j = P_\ell - P_K$$

$$\Delta P(f)_j = \frac{f_K \ell_K \phi_K \overline{W}_K^2}{Dh_K \overline{\rho}_K \overline{A}_K^2} + \frac{f_\ell \ell_\ell \phi_\ell \overline{W}_\ell^2}{Dh_\ell \overline{\rho}_\ell \overline{A}_\ell^2} + \frac{K_j W_j^2}{2\rho_j A_j^2}$$

$$\Delta P(z)_j = g_o\left[\overline{\rho}_K(\overline{Z}_K - Z_j) + \overline{\rho}_\ell(Z_j - \overline{Z}_\ell)\right]$$

and

$$\Delta P(s)_j = \frac{\overline{W}_K^2}{\overline{\rho}_K \overline{A}_K^2} - \frac{\overline{W}_\ell^2}{\overline{\rho}_\ell \overline{A}_\ell^2} - \frac{W_j^2}{2\rho_j}\left(\frac{1}{\overline{A}_K^2} - \frac{1}{\overline{A}_\ell^2}\right)$$

for simply connected volumes,

$$\Delta P(s)_{j1} = \frac{W_{j1}^2}{2\rho_{j1}}\left(\frac{1}{\bar{A}_{K1}^2} - \frac{1}{A_{j1}^2}\right) + \frac{W_m^2}{2\rho_m}\left(\frac{1}{A_m^2} - \frac{1}{\bar{A}_\ell^2}\right) + \frac{W_{j1}V_{j1} + W_{j2}V_{j2} - W_mV_m}{A_m}$$

for the drive flow junction, and

$$\Delta P(s)_{j2} = \frac{\bar{W}_{k2}^2}{\bar{\rho}_{k2}\bar{A}_{k2}^2} - \frac{W_{j2}^2}{\rho_{j2}A_{j2}^2} + \frac{W_{j2}^2}{2\rho_{j2}}\left(\frac{1}{A_{i2}^2} - \frac{1}{\bar{A}_{k2}^2}\right) + \frac{W_m^2}{2\rho_m}\left(\frac{1}{A_m^2} - \frac{1}{\bar{A}_\ell^2}\right)$$

$$+ \frac{W_{j1}V_{j1} + W_{j2}V_{j2} - W_mV_m}{A_m}$$

for the suction flow junction. At steady-state, the following mass flow rate relationships exist,

$$W_t = W_c + W_b \qquad \text{(C-5)}$$

$$W_t = W_r + W_p \qquad \text{(C-6)}$$

$$W_t = W_s + W_d \qquad \text{(C-7)}$$

and the junction and volume flow terms can be assigned to the above flow rates as

$$W_t = \bar{W}_1 = \bar{W}_4 = \bar{W}_5 = \bar{W}_6 = \bar{W}_8 = \bar{W}_9 = W_4 = W_5 = W_9$$

$$W_c = \bar{W}_2 = W_1 = W_2$$

$$W_b = \bar{W}_3 = W_3 = W_{10}$$

$$W_r = \bar{W}_7 = W_6 = W_7$$

$$W_p = \bar{W}_{12} = W_{14} = W_{15} = W_{16}$$

$$W_s = W_8$$

$$W_d = \bar{W}_{10} = \bar{W}_{11} = W_{12} = W_{13} = W_{11}$$

The simplified model contains three closed loop flow paths. At steady-state, the pressure drops summed around each of the closed loops must equal zero. The three loops are:

(1) Core loop - volumes 1, 2, 3, and 4

junctions 1, 2, 3, and 10

(2) Vessel loop - volumes 1, 2, 4, 5, 6, 7, 8 and 9

junctions 1, 2, 4, 5, 6, 7, 8 and 9

(3) Recirc. loop - volumes 8, 9, 10, and 11

junctions 8, 11, 12 and 13

Summing pressure drops around the core loop gives

$$\Delta P_1 + \Delta P_2 - \Delta P_{10} - \Delta P_3 = 0$$

and substituting for the ΔP's with Equation (C-1), grouping terms, and rearranging gives

$$\left[\frac{W_{10}^2}{2\rho_{10}}\left(\frac{1}{\bar{A}_1^2}-\frac{1}{\bar{A}_3^2}\right)+\frac{W_3^2}{2\rho_3}\left(\frac{1}{\bar{A}_3^2}-\frac{1}{\bar{A}_4^2}\right)-\frac{W_1^2}{2\rho_1}\left(\frac{1}{\bar{A}_1^2}-\frac{1}{\bar{A}_2^2}\right)-\frac{W_2^2}{2\rho_2}\left(\frac{1}{\bar{A}_2^2}-\frac{1}{\bar{A}_4^2}\right)\right.$$

$$+\frac{2f_3\ell_3\phi_3\bar{W}_3^2}{D_{h_3}\bar{\rho}_3\bar{A}_3^2}-\frac{2f_2\ell_2\phi_2\bar{W}_2^2}{D_{h_2}\bar{\rho}_2\bar{A}_2^2}+\frac{K_{10}W_{10}^2}{2\rho_{10}A_{10}^2}+\frac{K_3W_3^2}{2\rho_3A_3^2}-\frac{K_1W_1^2}{2\rho_1A_1^2}-\frac{K_2W_2^2}{2\rho_2A_2^2}$$

$$\left.+g_c\left(\bar{\rho}_2(Z_1-Z_2)-\bar{\rho}_3(Z_{10}-Z_3)\right)\right]=0$$

This equation can be expressed in terms of the core and bypass flows and the elevation term as

$$W_b^2\left[\frac{1}{2\rho_{10}}\left(\frac{1}{\bar{A}_1^2}-\frac{1}{\bar{A}_3^2}\right)+\frac{1}{2\rho_3}\left(\frac{1}{\bar{A}_3^2}-\frac{1}{\bar{A}_4^2}\right)+\frac{2f_3\ell_3\phi_3}{D_{h_3}\bar{\rho}_3\bar{A}_3^2}+\frac{K_{10}}{2\rho_{10}A_{10}^2}+\frac{K_3}{2\rho_3A_3^2}\right]$$

$$-W_c^2\left[\frac{1}{2\rho_1}\left(\frac{1}{\bar{A}_1^2}-\frac{1}{\bar{A}_2^2}\right)+\frac{1}{2\rho_2}\left(\frac{1}{\bar{A}_2^2}-\frac{1}{\bar{A}_4^2}\right)+\frac{2f_2\ell_2\phi_2}{D_{h_2}\bar{\rho}_2\bar{A}_2^2}+\frac{K_1}{2\rho_1A_1^2}+\frac{K_2}{2\rho_2A_2^2}\right]$$

$$+g_0\left[\bar{\rho}_2(Z_1-Z_2)-\bar{\rho}_3(Z_{10}-Z_3)\right]=0$$

Assigning representative terminology to the bracketed terms,

$$\Theta_1=\left[\frac{1}{2\rho_{10}}\left(\frac{1}{\bar{A}_1^2}-\frac{1}{\bar{A}_3^2}\right)+\frac{1}{2\rho_3}\left(\frac{1}{\bar{A}_3^2}-\frac{1}{\bar{A}_4^2}\right)+\frac{2f_3\ell_3\phi_3}{D_{h_3}\bar{\rho}_3\bar{A}_3^2}+\frac{K_{10}}{2\rho_{10}A_{10}^2}+\frac{K_3}{2\rho_3A_3^2}\right]$$

$$\Theta_2=\left[\frac{1}{2\rho_1}\left(\frac{1}{\bar{A}_1^2}-\frac{1}{\bar{A}_2^2}\right)+\frac{1}{2\rho_2}\left(\frac{1}{\bar{A}_2^2}-\frac{1}{\bar{A}_4^2}\right)+\frac{2f_2\ell_2\phi_2}{D_{h_2}\bar{\rho}_2\bar{A}_2^2}+\frac{K_1}{2\rho_1A_1^2}+\frac{K_2}{2\rho_2A_2^2}\right]$$

$$\Theta_3=g_0\left[\bar{\rho}_2(Z_1-Z_2)+\bar{\rho}_3(Z_{16}-Z_3)\right]$$

thus reduces the equation to

$$\Theta_1W_b^2-\Theta_2W_c^2+\Theta_3=0$$

Now substitute for the core flow using Equation (C-5), resulting in the following equation in terms of W_b and W_t:

$$(\Theta_1-\Theta_2)W_b^2+(2\Theta_2W_t)W_b+(\Theta_3-\Theta_2W_t^2)=0$$

This equation can be solved for the bypass flow as a function of the

total flow, giving

$$W_b = \frac{-2\theta_2 W_t \pm \sqrt{(2\theta_2 W_t)^2 - 4(\theta_1 - \theta_2)(\theta_3 - \theta_2 W_t^2)}}{2(\theta_1 - \theta_2)}$$

Repeating this process for the vessel loop gives

$$\Delta P_1 + \Delta P_2 + \Delta P_4 + \Delta P_5 + \Delta P_6 + \Delta P_7 + \Delta P_8 + \Delta P_9 = 0$$

and using equations (C-1) and (C-3) plus the steady-state flow relationships yields

$$W_t^2 \left[\frac{1}{2\rho_m}\left(\frac{1}{A_m^2} - \frac{1}{\bar{A}_9^2}\right) - \frac{1}{2\rho_4}\left(\frac{1}{\bar{A}_4^2} - \frac{1}{\bar{A}_5^2}\right) - \frac{1}{2\rho_5}\left(\frac{1}{\bar{A}_5^2} - \frac{1}{\bar{A}_6^2}\right) - \frac{1}{2\rho_9}\left(\frac{1}{\bar{A}_9^2} - \frac{1}{\bar{A}_1^2}\right) \right.$$

$$+ \frac{1}{\bar{\rho}_9 \bar{A}_9^2} - \frac{1}{\rho_m A_m^2} - \frac{2f_1 l_1 \phi_1}{D_{h_1} \bar{\rho}_1 \bar{A}_1^2} - \frac{2f_4 l_4 \phi_4}{D_{h_4} \bar{\rho}_4 \bar{A}_4^2} - \frac{2f_5 l_5 \phi_5}{D_{h_5} \bar{\rho}_5 \bar{A}_5^2} - \frac{2f_6 l_6 \phi_6}{D_{h_6} \bar{\rho}_6 \bar{A}_6^2}$$

$$\left. - \frac{2f_8 l_8 \phi_8}{D_{h_8} \bar{\rho}_8 \bar{A}_8^2} - \frac{2f_9 l_9 \phi_9}{D_{h_9} \bar{\rho}_9 \bar{A}_9^2} - \frac{K_4}{2\rho_4 A_4^2} - \frac{K_5}{2\rho_5 A_5^2} - \frac{K_9}{2\rho_9 A_9^2} \right]$$

$$- W_c^2 \left[\frac{1}{2\rho_1}\left(\frac{1}{\bar{A}_1^2} - \frac{1}{\bar{A}_2^2}\right) + \frac{1}{2\rho_2}\left(\frac{1}{\bar{A}_2^2} - \frac{1}{\bar{A}_4^2}\right) + \frac{2f_2 l_2 \phi_2}{D_{h_2} \bar{\rho}_2 \bar{A}_2^2} + \frac{K_1}{2\rho_1 A_1^2} + \frac{K_2}{2\rho_2 A_2^2} \right]$$

$$- W_r^2 \left[\frac{1}{2\rho_6}\left(\frac{1}{\bar{A}_6^2} - \frac{1}{\bar{A}_7^2}\right) + \frac{1}{2\rho_7}\left(\frac{1}{\bar{A}_7^2} - \frac{1}{\bar{A}_8^2}\right) + \frac{2f_7 l_7 \phi_7}{D_{h_7} \bar{\rho}_7 \bar{A}_7^2} + \frac{K_6}{2\rho_6 A_6^2} + \frac{K_7}{2\rho_7 A_7^2} \right]$$

$$+ W_s^2 \left[\frac{1}{2\rho_8}\left(\frac{1}{A_8^2} - \frac{1}{\bar{A}_8^2}\right) + \frac{1}{\rho_8 A_8 A_m} - \frac{1}{\rho_8 A_8^2} - \frac{K_8}{2\rho_8 A_8^2} \right] + W_d^2 \left[\frac{1}{\rho_{13} A_{13} A_m} \right]$$

$$+ g_o \left[\bar{\rho}_1 (Z_9 - Z_1) + \bar{\rho}_2 (Z_1 - Z_2) + \bar{\rho}_4 (Z_2 - Z_4) + \bar{\rho}_5 (Z_4 - Z_5) \right.$$

$$\left. + \bar{\rho}_6 (Z_5 - Z_6) + \bar{\rho}_7 (Z_6 - Z_7) + \bar{\rho}_8 (Z_7 - Z_8) + \bar{\rho}_9 (Z_8 - Z_9) \right] = 0$$

Making similar substitutions for the bracketed terms results in

$$\theta_4 W_t^2 - \theta_5 W_c^2 - \theta_6 W_r^2 + \theta_7 W_s^2 + \theta_8 W_d + \theta_9 = 0$$

where the θ terms are equal to the corresponding expressions in the preceding equation. Substituting for the drive flow using Equation (C-7) gives

$$(\theta_7 + \theta_8) W_s^2 - (2\theta_8 W_t) W_s + ((\theta_4 + \theta_8) W_t^2 - \theta_5 W_c^2 - \theta_6 W_r^2 + \theta_9) = 0$$

With the core flow determined by Equations (C-8) and (C-5), and the recirculation flow known assuming that the total and steam flows are known (by Equation (C-6)), this equation relates the suction flow to the total flow. Solving for the suction flow gives

$$W_s = \frac{2\theta_8 W_t \pm \sqrt{(2\theta_8 W_t)^2 - 4(\theta_7 + \theta_8)((\theta_4 + \theta_8) W_t^2 - \theta_5 W_c^2 - \theta_6 W_r^2 + \theta_9)}}{2(\theta_7 + \theta_8)}$$

For the final closed loop, the recirculation system, summing the pressure drops results in

$$\Delta P_8 - \Delta P_{11} - \Delta P_{12} - \Delta P_{13} = 0$$

and substituting using Equations (C-1), (C-2) and (C-3) along with the steady-state flow relationships, grouping terms, and rearranging gives

$$W_s^2\left[\frac{1}{2\rho_8}\left(\frac{1}{A_8^2}-\frac{1}{\bar{A}_8^2}\right)-\frac{1}{\rho_8 A_8^2}-\frac{K_8}{2\rho_8 A_8^2}\right]+W_d^2\left[\frac{1}{2\rho_{11}}\left(\frac{1}{\bar{A}_8^2}-\frac{1}{\bar{A}_{10}^2}\right)\right.$$

$$+\frac{1}{2\rho_{12}}\left(\frac{1}{\bar{A}_{10}^2}-\frac{1}{\bar{A}_{11}^2}\right)-\frac{1}{2\rho_{13}}\left(\frac{1}{\bar{A}_{11}^2}-\frac{1}{A_{13}^2}\right)+\frac{1}{\bar{\rho}_{11}\bar{A}_{11}^2}+\frac{2f_{10}\ell_{10}\phi_{10}}{D_{h10}\bar{\rho}_{10}\bar{A}_{10}^2}+\frac{2f_{11}\ell_{11}\phi_{11}}{D_{h11}\bar{\rho}_{11}\bar{A}_{11}^2}$$

$$\left.+\frac{K_{11}}{2\rho_{11}A_{11}^2}+\frac{K_{12}}{2\rho_{12}A_{12}^2}+\frac{K_{13}}{2\rho_{13}A_{13}^2}\right]+g_c\left[\bar{\rho}_8(Z_{11}-Z_8)+\bar{\rho}_9(Z_8-Z_{13})\right.$$

$$\left.-\bar{\rho}_{10}(Z_{11}-Z_{12})-\bar{\rho}_{11}(Z_{12}-Z_{13})\right]=\Delta P_{pump}(144g_c)$$

Using the pump head approximation developed in Appendix B and assigning constants after grouping like terms results in

$$\Theta_{10}W_s^2+\Theta_{11}W_d^2+\Theta_{12}=\Theta_{13}W_d\alpha$$

where

$$\Theta_{10}=\left[\frac{1}{2\rho_8}\left(\frac{1}{A_8^2}-\frac{1}{\bar{A}_8^2}\right)-\frac{1}{\rho_8 A_8^2}-\frac{K_8}{2\rho_8 A_8^2}\right]$$

$$\Theta_{11}=\left[\frac{1}{2\rho_{11}}\left(\frac{1}{\bar{A}_8^2}-\frac{1}{\bar{A}_{10}^2}\right)+\frac{1}{2\rho_{12}}\left(\frac{1}{\bar{A}_{10}^2}-\frac{1}{\bar{A}_{11}^2}\right)-\frac{1}{2\rho_{13}}\left(\frac{1}{\bar{A}_{11}^2}-\frac{1}{A_{13}^2}\right)+\frac{1}{\bar{\rho}_{11}\bar{A}_{11}^2}\right.$$

$$+\frac{2f_{10}\ell_{10}\phi_{10}}{D_{h10}\bar{\rho}_{10}\bar{A}_{10}^2}+\frac{2f_{11}\ell_{11}\phi_{11}}{D_{h11}\bar{\rho}_{11}\bar{A}_{11}^2}+\frac{K_{11}}{2\rho_{11}A_{11}^2}+\frac{K_{12}}{2\rho_{12}A_{12}^2}+\frac{K_{13}}{2\rho_{13}A_{13}^2}$$

$$\left.-\frac{g_o b\beta^2 H_r}{V_r^2\bar{\rho}_{10}}\right]$$

$$\theta_{12} = g_o\left[\bar{\rho}_8(Z_{11}-Z_8) + \bar{\rho}_9(Z_8-Z_{13}) - \bar{\rho}_{10}(Z_{11}-Z_{12}) - \bar{\rho}_{11}(Z_{12}-Z_{13})\right]$$

$$\theta_{13} = \frac{g_o m \beta H r}{V_r}$$

and solving the equation for the normalized pump speed (α) gives

$$\alpha = \frac{\theta_{10} W_s^2 + \theta_{11} W_d + \theta_{12}}{\theta_{13} W_d}$$

Equations (C-5) through (C-10) form the simplified model solution which relates the pump speed to the flow rates under the assumption that the steam and total flow are known, and the θ terms are constants.

The physical constants from the RETRAN model as used for evaluating the θ terms are tabulated in Table C-1. The only adjustments required for these terms are for the core volume, where the 12-volume core parameters from the RETRAN model are adapted to the single core volume in the simplified model. The densities are taken from the steady-state equilibrium conditions generated by RETRAN for the reference case. This steady-state data is also used for hand calculations of the friction factors, using correlations found in Reference 5. These are also tabulated in Table C1 and, as was the case for the physical constants for the core volume, the density and friction factors for the core are based on average conditions over the RETRAN core volumes.

Using the data in Table C1, the θ terms were calculated, and a test case for reference conditions was used to determine the proper

signs in the quadratic solutions of Equations (C-8) and (C-9). These results are presented in Table C2, along with a comparison with the RETRAN results for the reference case.

The final simplified model solution is now determined to be

(1) Select W_t, W_p

(2) $$W_b = \frac{-2\Theta_2 W_t + \sqrt{(2\Theta_2 W_t)^2 - 4(\Theta_1 - \Theta_2)(\Theta_3 - \Theta_2 W_t^2)}}{2(\Theta_1 - \Theta_2)}$$

(3) $$W_c = W_t - W_b$$

$$W_r = W_t - W_p$$

(4) $$W_s = \frac{2\Theta_8 W_t - \sqrt{(2\Theta_8 W_t)^2 - 4(\Theta_7 + \Theta_8)((\Theta_4 + \Theta_8)W_t^2 - \Theta_5 W_c^2 - \Theta_6 W_r^2 + \Theta_9)}}{2(\Theta_7 + \Theta_8)}$$

(5) $$W_d = W_t - W_s$$

(6) $$\alpha = \frac{\Theta_{10} W_s^2 + \Theta_{11} W_d^2 + \Theta_{12}}{\Theta_{13} W_d}$$

Table C1. Input Data for Calculation of the Constants in the Simplified Model.

Vol.	Flow Area (ft^2)	Flow Length (ft)	Hyd. Diameter (ft)	Density (lb/ft^3)	Friction Factor	Two-Phase Fric. Factor	Elevation (ft)
1	115.8664	18.2465	0.16472	47.5022	0.00318	1.0	9.0130
2	82.4216	12.0000	0.04834	28.5642	0.00376	2.52376	24.0260
3	35.3603	12.0000	0.10511	47.1460	0.00438	1.0	24.0260
4	206.6750	5.6000	0.03237	13.2442	0.00485	5.37726	32.8269
5	42.3323	6.8333	0.50542	13.1021	0.00223	3.55426	39.0445
6	42.3323	23.1439	0.50542	23.7473	0.00223	2.18584	46.5417
7	226.2395	8.1667	1.78000	26.5431	0.00243	2.60469	46.5417
8	132.5028	32.2917	1.20580	47.5083	0.00234	1.0	26.3921
9	39.3790	6.0015	0.03883	47.5020	0.00341	1.0	18.4000
10	7.8056	75.9831	2.22917	47.5203	0.00168	1.0	-6.2292
11	8.0654	76.9857	1.03890	47.5681	0.00187	1.0	2.9623

Table C1. (Cont.)

Jun.	Flow Area (ft^2)	Loss Coefficient	Density (lb/ft^3)	Elevation (ft)	100% Flows (lb/sec)
1	82.4216	32.16786	47.5010	18.0260	26011.8
2	82.4216	4.09279	12.3364	30.0260	26011.8
3	35.0686	96.09	46.8022	30.0260	2460.4
4	42.3323	0.359	13.2287	35.6278	28472.2
5	42.3323	0.449	13.0896	42.4583	28472.2
6	122.9047	0.0	45.0081	42.4583	24755.4
7	293.1067	0.0	45.6892	42.4583	24755.4
8	6.2235	0.581329	47.5082	26.4741	19453.1
9	39.3790	0.875	47.5023	10.3258	28472.2
10	35.0686	983.9316	47.5010	18.0260	2460.4
11	7.8056	0.85	47.5100	12.3438	9019.1
12	7.8056	4.938	47.5222	-22.69792	9019.1
13	1.0755	0.32643	47.5647	26.4741	9019.1
m	7.2990	---	47.5261		28472.2

Table C2. Constant Values and Reference Case Comparison

Constant (θ)	Reference Value
1	9.274237 E-3
2	9.353638 E-5
3	7.174210 E+3
4	-2.276909 E-4
5	9.353638 E-5
6	5.597228 E-6
7	3.308722 E-5
8	2.678190 E-3
9	1.387381 E+4
10	-4.302886 E-4
11	3.292020 E-2
12	8.092516 E+1
13	3.024015 E+2

Flow Term	Approximate Value	RETRAN Value
W_t	28472.2	28472.2
W_p	3716.8	3716.8
W_c	26012.4	26011.8
W_c	2459.8	2460.4
W_r	24755.4	24755.4
W_s	19455.7	19453.1
W_d	9016.5	9019.1
α	0.9219	0.9247